https://doi.org/10.5194/tc-2022-105
Preprint. Discussion started: 31 May 2022

The Cryosphere Discussions

The stability of present-day Antarctic grounding lines — Part B: Possible commitment of regional collapse under current climate

Ronja Reese[1,2], Julius Garbe[2,3], Emily A. Hill[1], Benoît Urruty[4], Kaitlin A. Naughten[5], Olivier Gagliardini[4], Gael Durand[4], Fabien Gillet-Chaulet[4], David Chandler[6], Petra M. Langebroek[6], and Ricarda Winkelmann[2,3]

[1]Department of Geography and Environmental Sciences, Northumbria University, Newcastle, UK
[2]Potsdam Institute for Climate Impact Research (PIK), Member of the Leibniz Association, Potsdam, Germany
[3]Institute of Physics and Astronomy, University of Potsdam, Potsdam, Germany
[4]Univ. Grenoble Alpes, CNRS, IRD, Grenoble INP, IGE, 38000 Grenoble, France
[5]British Antarctic Survey, Cambridge, UK
[6]NORCE Norwegian Research Centre, Bjerknes Centre for Climate Research, Bergen, Norway

Correspondence: Ronja Reese (ronja.reese@northumbria.ac.uk)

Abstract. Observations of ocean-driven grounding line retreat in the Amundsen Sea Embayment in Antarctica give rise to the question of a collapse of the West Antarctic Ice Sheet. Here we analyse the committed evolution of Antarctic grounding lines under present-day climate conditions to locate the underlying steady states that they are attracted to and understand the reversibility of large-scale changes. To this aim, we first calibrate the sub-shelf melt module PICO with observed and modelled melt sensitivities to ocean temperature changes. Using the new calibration, we run an ensemble of historical simulations from 1850 to 2015 with the Parallel Ice Sheet Model to create model instances of possible present-day ice sheet configurations. Then, we extend a subset of simulations best representing the present-day ice sheet for another 10,000 years to investigate their evolution under constant present-day climate forcing. We test for reversibility of grounding line movement if large-scale retreat occurs. While we find parameter combinations for which no retreat happens in the Amundsen Sea Embayment sector, we also find admissible model parameters for which an irreversible retreat takes place. Hence, it cannot be ruled out that the grounding lines – which are not engaged in an irreversible retreat at the moment as shown in our companion paper (Part A, Urruty et al., subm.) – will evolve towards such a retreat under current climate conditions. Importantly, an irreversible collapse in the Amundsen Sea Embayment sector evolves on millennial timescales and is not inevitable yet, but could become so if forcing on the climate system is not reduced in the future. In contrast, we find that allowing ice shelves to regrow to their present geometry means that large-scale grounding line retreat into marine basins upstream of Filchner-Ronne and Ross ice shelves is reversible. Other grounding lines remain close to their current positions in all configurations under present-day climate.

1 Introduction

The potential for the West Antarctic Ice Sheet (WAIS) to collapse in response to global warming was first raised as a concern in Mercer (1978). This collapse would be driven by the Marine Ice Sheet Instability (MISI; Weertman, 1974; Schoof, 2007, 2012) and would raise global sea-levels by more than 3 meters in the long term. Over the past decades, the Antarctic Ice Sheet has

https://doi.org/10.5194/tc-2022-105
Preprint. Discussion started: 31 May 2022

been losing mass (Smith et al., 2020) at an increasing rate (Shepherd et al., 2018; Rignot et al., 2019) with current mass losses being driven by buttressing loss of ice shelves through increased ocean-driven melting (Paolo et al., 2015). In particular, retreat of grounding lines – the boundary separating the grounded parts of the ice sheet from its floating ice shelves – and increased mass loss in the Amundsen Sea Embayment (ASE) sector (Rignot et al., 2019; Milillo et al., 2022) have raised the question of whether a collapse of the West Antarctic Ice Sheet driven by MISI might already be underway (Rignot et al., 2014; Joughin et al., 2014; Favier et al., 2014). Several numerical modelling studies find continued retreat in the ASE under current climate conditions (Joughin et al., 2014; Favier et al., 2014; Seroussi et al., 2017; Arthern and Williams, 2017) and also the commitment of large-scale retreat was found possible close to present-day climate conditions: Garbe et al. (2020) report that retreat of West Antarctic grounding lines could be initiated by around $1-2$ °C of global warming above pre-industrial and Golledge et al. (2021) find that in a simulation coming from the last interglacial, the West Antarctic Ice Sheet starts retreating after 1500 years with constant current climate conditions. These findings raise the importance of a systematic analysis to identify whether Antarctic grounding lines are *currently* engaged in an irreversible retreat due to MISI, and a more detailed understanding of the committed retreat under present-day climate conditions, i.e., the steady state positions that current grounding lines are attracted to and the (ir)reversibility of potential large-scale transitions. Here and in an accompanying paper (Part A, Urruty et al., subm.) we address these questions.

Urruty et al. (subm.) show that present-day Antarctic grounding line retreat is likely a 'forced retreat', meaning it is driven by external forcing alone rather than by the MISI instability mechanism at the moment. That no irreversible retreat is found in the current Antarctic geometry could be explained by two different underlying stability regimes of the system. Either MISI is in principle existent but not at play, or MISI is generally suppressed. The latter has been found to be the case in the presence of strong ice-shelf buttressing (Gudmundsson et al., 2012; Pegler, 2018; Haseloff and Sergienko, 2018). The existence of tipping points due to MISI is thus a priori not clear for buttressed Antarctic grounding lines located on retrograde bed slopes. The potential for irreversible grounding-line retreat in regions upstream of present-day grounding lines has been shown in numerical simulations for the whole Antarctic Ice Sheet (Garbe et al., 2020), the West Antarctic Ice Sheet (Feldmann and Levermann, 2015), the Wilkes subglacial basin in East Antarctica (Mengel and Levermann, 2014), and using high resolution modelling with an in-depth tipping analysis for Pine Island Glacier in the ASE sector (Rosier et al., 2021). The existence of tipping points for other grounding lines requires further investigation.

In this paper, we analyse the current trend in Antarctic grounding lines – observations show that they are clearly not in steady state at the moment – by investigating to which steady state positions grounding lines evolve towards under current climate conditions. If we find that the current climate commits grounding lines to large-scale retreat, we test if this retreat is reversible. To do so, constant present-day climate is applied in the simulations and no future changes in the climate conditions are included. This means that the simulations are not projections, but rather allow us to assess the commitment of grounding line retreat under continued current climate forcing. We discuss the possible ice sheet states and stability regimes in more detail in Section 2.

Firstly, we create a set of plausible model representations of the Antarctic Ice Sheet with the Parallel Ice Sheet Model (PISM). They are forced from 1850 to 2015 by historic changes in the ocean and atmosphere from a simulation of the Coupled

https://doi.org/10.5194/tc-2022-105
Preprint. Discussion started: 31 May 2022

Model Intercomparison Project Phase 5 to ensure that they replicate the present-day trend in mass loss. Sub-shelf melt rates are calculated using the Potsdam Ice shelf Cavity mOdel (PICO; Reese et al., 2018a). Observed ongoing retreat in the ASE sector is linked to oceanic forcing (Jenkins et al., 2018) and recent projections underline the importance of the sensitivity of sub-shelf melting to ocean temperature variations (Jourdain et al., 2020; Seroussi et al., 2020; Reese et al., 2020). We thus calibrate the sub-shelf melt module PICO to represent observed (Jenkins et al., 2018) or modelled (Naughten et al., 2021) sensitivities of melt rates to ocean temperature changes. This is described in Section 3.

We then let the ice sheet states evolve under constant present-day climate conditions towards steady state and evaluate the corresponding committed grounding line movement. Note that a steady state reached this way is by construction stable. Also these experiments do not answer whether MISI is *currently* underway for Antarctic grounding lines but they instead explore whether an irreversible retreat might be committed to occur eventually under present-day climate conditions. To test for (ir)reversibility of grounding line retreat, we revert the climate conditions to pre-industrial and extend the simulations that show grounding line retreat by $20,000$ years. These experiments are presented in Section 4.

The results are then discussed in Section 5 and summarised in Section 6.

2 Theoretical framing

We here discuss the potential states that Antarctic grounding lines could be in with respect to MISI. The terminology used for nonlinear systems is based on Strogatz (2018).

MISI occurs when a positive feedback, where retreat of the grounding line increases the ice flow across the grounding line and this in turn causes further retreat, is at play. For a laterally uniform ice sheet, ice flow across the grounding line is a function of the local ice thickness which is linked through the flotation criterion to the bed topography. This means that due to the positive feedback, stable steady state grounding-line positions cannot exist on retrograde, in-land sloping beds (for constant bed properties and ice rheology; Schoof, 2007, 2012). In the presence of buttressing ice shelves, conditions are more complicated and it is possible that no MISI exists (Gudmundsson et al., 2012; Haseloff and Sergienko, 2018; Pegler, 2018). In the absence of buttressing, it was found that also a specific distribution of the basal friction parameter can allow for stable steady state grounding lines on retrograde sloping beds Brondex et al. (2017). Numerical modelling is then required to assess the state of the grounding lines.

MISI gives rise to hysteresis behaviour (Schoof, 2007) which can be visualised in a bifurcation diagram showing the system state, i.e., current location of the grounding line, with respect to the relevant control parameter, i.e., climate forcing in the atmosphere and ocean, see Fig. 1. Hysteresis means that over a range of control parameters, several possible steady states exist and thus the (evolution of the) current system state depends on its history. Those steady states can be stable or unstable, depending on whether a small-amplitude perturbation to the system is dampened (stable) or amplified (unstable) so that the system evolves back to its original steady state or away from it. At a bifurcation, or tipping point, a stable and an unstable branch merge, and if the system is moved beyond that point, it will engage in an irreversible transition towards the only existing stable state. Moving the system across a tipping point by changes in the control parameter is how tipping in marine

https://doi.org/10.5194/tc-2022-105
Preprint. Discussion started: 31 May 2022

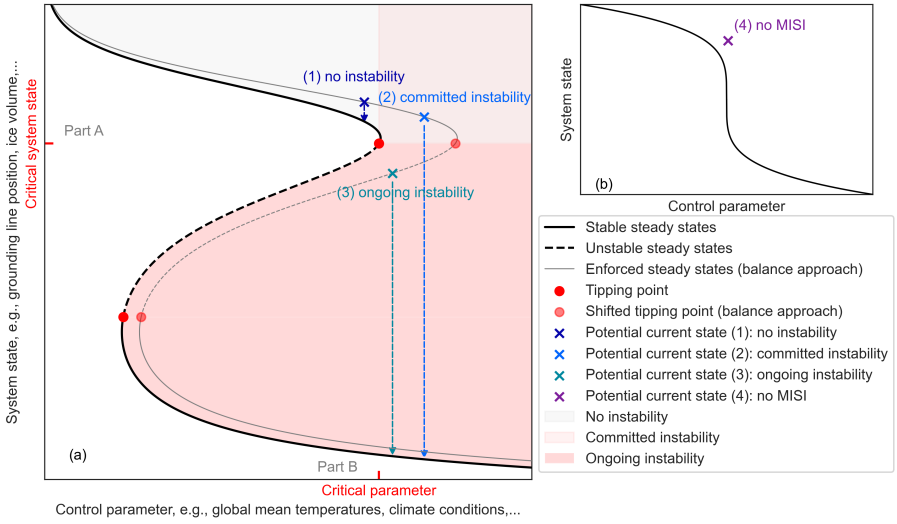

Figure 1. Schematic of potential stability regimes of Antarctic grounding lines. Illustrated are possible present-day states of Antarctic grounding lines in (a) a schematic bifurcation diagram for the Marine Ice Sheet Instability and (b) a schematic diagram illustrating a fully reversible system, both represented by a system state and a control parameter. Black curve shows underlying steady system states (solid for stable, dashed for unstable). Tipping points or bifurcation points (red points) lie at the critical control parameter and critical system state. If MISI exists (panel a), the current, non-steady grounding line (indicated by crosses) might be at three qualitatively different locations relative to the steady-state curve and the tipping point. If no MISI exists (panel b), large-scale changes in the system state are reversible. In the companion paper, Part A (Urruty et al., subm.), is is assessed whether the grounding line is currently undergoing MISI, by enforcing a steady state using a balanced-melt approach (grey curve). In this paper, Part B, we analyse the long-term evolution of the grounding lines (indicated by arrows) and their reversibility, i.e., whether large-scale retreat might be committed under constant climate forcing and if so, if this retreat is reversible.

ice sheets is generally thought to occur (this is called bifurcation-induced tipping, alternative ways that tipping can occur are discussed for example in Vanselow et al. (2022)). Such a transition is called 'irreversible', since reverting back to the original state requires the control parameter to be reduced substantially below the critical value until a second tipping point is crossed and the system irreversibly changes back to the first state. See Rosier et al. (2021) for a more detailed discussion.

Grounding lines in Antarctica show 'slow-onset' tipping (Ritchie et al., 2021) since also under very slowly increasing control parameters in quasi-steady experiments the ice sheet's system state was found to evolve above the equilibrium curve, see Garbe et al. (2020) and Rosier et al. (2021). This means that crossing a critical threshold in their forcing (i.e., climate conditions) does not directly lead to an irreversible change in the their state (e.g., WAIS collapse). Instead, it is possible to have a temporary overshoot over the critical threshold without forcing the grounding lines to enter irreversible retreat (a relationship between time and amplitude for safe overshoots is derived for simple systems in Ritchie et al., 2019). Such states have been described as affording 'borrowed time' in which it is possible to revert to previous conditions before the undesirable system state locks in (Hughes et al., 2013). This is in line with Rosier et al. (2021) showing that critical slowing for MISI – which is a typical

https://doi.org/10.5194/tc-2022-105
Preprint. Discussion started: 31 May 2022

response for such a system approaching a tipping point (see also Scheffer et al., 2009) – only occurs when the critical system state is crossed, not the critical control parameter. It is also plausible since the mechanical, positive feedback related to MISI only kicks in once the critical system state (grounding line position) is crossed.

To summarise, present-day Antarctic grounding lines can either show no hysteresis behaviour (Fig. 1b), or, if hysteresis exists, they are in a transient state above or right of the upper stable branch of the underlying equilibrium curve (Fig. 1a, note that we focus on the upper stable branch here since we consider upstream tipping points). In the latter case, this means that an ice sheet, in particular under realistic forcing, does not necessarily cross the critical control parameter (i.e., climate conditions) and the critical system state (i.e., grounding line position) of a tipping point simultaneously.

Current grounding lines can hence be in principle in four qualitatively different positions in terms of MISI (see Fig. 1):

1. **No instability:** MISI exists, and the grounding line has neither crossed the critical system state nor the critical control parameter. Letting the grounding line evolve with the control parameter kept constant, it would reach a stable steady state on the upper stable branch (following the dark blue arrow), and no tipping occurs.

2. **Committed instability:** MISI exists, and the grounding line has crossed the critical control parameter, but not the critical system state. It is in an 'overshoot' state, i.e., it will evolve to the lower stable steady state branch but the collapse could still be prevented by reducing the control parameter below its critical value. However, if the control parameter is kept constant, it will eventually cross the critical system state and enter irreversible retreat (following the light blue arrow). Such a state is hence showing no instability at the moment, but an instability, or tipping, is committed under a constant control parameter.

3. **Ongoing instability:** MISI exists, and the current grounding line has crossed the critical parameter and the critical system state. Such a state is undergoing irreversible retreat. Evolving this system forward under constant climate conditions the grounding line would, similar to the second case, retreat further until it reaches a new stable steady state (following the teal arrow). Such a state is considered to be tipped.

4. **No MISI:** MISI is suppressed. The system might show large-scale changes for small changes in the control parameter, but these are reversible.

The numerical stability analysis of our companion paper (Urruty et al., subm.) analyses whether MISI is currently happening for any Antarctic grounding line. In that paper, a balance approach is used by which the surface mass balance is modified so that the current Antarctic grounding lines are in steady state (indicated by the grey curve in Fig. 1). Then, their stability is tested in a numerical stability analysis. If a stable steady state is found with respect to the modified surface mass balance, then the grounding line is likely not undergoing MISI in its current position or no MISI exists. But if an unstable steady state is found, then the grounding line is likely undergoing MISI in its current position. The study hence analyses the position of current Antarctic grounding lines with respect to the critical system state. Its findings can be interpreted to show that either case (1), (2) or (4) are likely true for all Antarctic grounding lines, and that case (3) can be excluded. Note that with this methodology, case (1), (2) or (4) cannot be distinguished.

https://doi.org/10.5194/tc-2022-105
Preprint. Discussion started: 31 May 2022

The present paper can be understood to investigate the question whether the current Antarctic Ice Sheet is more likely to represent case (1), (2) or (4), i.e., whether present-day climate forcing commits the grounding lines to substantially retreat away from their current positions, or if they remain close to their current states. And if they retreat, if this retreat is reversible. In other words, this paper analyses the position of current Antarctic grounding lines with respect to the critical control parameter (i.e., climate conditions).

3 PICO parameter optimization

In this section, we introduce a new optimisation approach for the parameters in the PICO model in order to obtain suitable values for Antarctic model simulations, including projections of Antarctica's future sea level contribution. We first describe the methodology, see Sect. 3.1, then the melt sensitivity estimates for the Filchner-Ronne Ice Shelf (FRIS) and the Amundsen Sea ice shelves, see Sect. 3.2, that are used as targets to select the PICO parameters in Sect. 3.3. We then use this parameter set for all simulations conducted in this paper, using the ice sheet model PISM to investigate the commitment of grounding line retreat under present-day climate conditions.

3.1 PICO model

PICO calculates sub-shelf melt rates in ice-shelf cavities based on far-field ocean temperature and salinity. It extends the ocean box model (Olbers and Hellmer, 2010) for application in ice sheet models that resolve both horizontal dimensions. We provide far-field ocean temperatures and salinities to PICO which differ in between 19 basins surrounding the Antarctic Ice Sheet and are derived from Schmidtko et al. (2014), similar to Reese et al. (2018a).

PICO parameterises the vertical overturning circulation in ice shelf cavities and includes a formulation of the ice-ocean boundary layer. For each of these processes, PICO has one parameter, which is constant across all Antarctic ice shelves. The parameter C influences the strength of the vertical overturning circulation, and the parameter $\gamma_T^\star$ describes the vertical heat exchange coefficient at the ice-ocean interface, which in reality depends on the ocean velocity and the ice roughness. In this paper we present a new optimization approach in which these parameters are selected such that the modelled sensitivity matches the sensitivity of melt rates to ocean temperature changes obtained from observations or numerical ocean modelling. In the following section we describe these targets and then present the parameter optimization in the section afterwards.

3.2 Target melt sensitivity for Filchner-Ronne Ice Shelf and the Amundsen Sea Region

An analytical model of the ice-ocean interface (Jenkins et al., 2018) and numerical models of idealised ice shelf cavities (Holland et al., 2008) suggests a quadratic dependency of ice shelf melting on ocean temperature changes. Temperature changes can equivalently be expressed in terms of thermal driving that is defined as the temperature above freezing point determined by local salinity and a reference pressure value, and both are used hereafter. For simplicity we use the surface freezing point, as the ice shelf draft (and therefore the in-situ freezing point) varies both in space and time.

https://doi.org/10.5194/tc-2022-105
Preprint. Discussion started: 31 May 2022

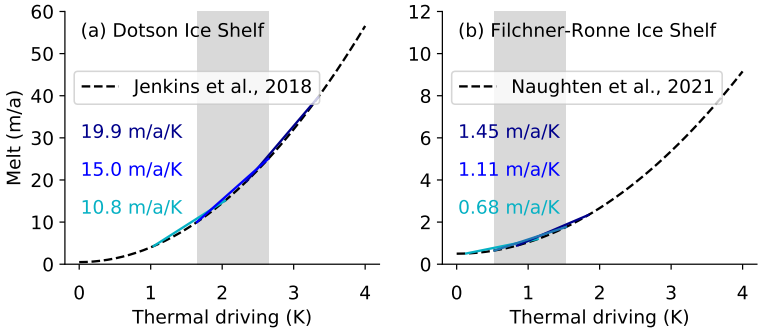

Figure 2. Target sensitivities for (a) Dotson Ice Shelf and (b) Filchner-Ronne Ice Shelf. Thermal driving is given relative to the surface freezing point and represents properties of the water masses at depth on the continental shelf in front of the ice shelf cavity. Melt is average melt rate over the ice shelf in meter ice-equivalent per year. Dashed lines indicate estimations by Jenkins et al. (2018) and based on Naughten et al. (2021) as detailed in Appendix A1. Grey bar indicates range over which linear sensitivity is approximated, using present-day thermal driving for the baseline temperatures. Coloured lines and numbers show the maximum, mean and minimum linear sensitivity estimates depending on the choice of present-day baseline temperatures (see Appendix A2).

We use the quadratic relationship between melt rates and ocean temperatures obtained from observational data for Dotson Ice Shelf (Jenkins et al., 2018) as a target for the Amundsen Sea, see Fig. 2a. Doing so, we hope to represent the sensitivity correctly for small, warm cavities. For cold, large cavities, no observations spanning such a wide range of temperature inputs are available. Instead we use recent numerical ocean model simulations that include a switch from cold to warm conditions in the Filchner-Ronne Ice Shelf cavity (Naughten et al., 2021) and estimate a quadratic relationship from these, see Fig. 2b, with the procedure described in detail in Appendix A1.

To get a sensitivity target for tuning PICO, we linearise the curves around present-day ocean temperatures. Note that PICO shows a linear sensitivity in particular for higher temperatures, because melting in PICO depends linearly on thermal driving and no dependency on the overturning velocity (which is also a function of thermal driving) is included in PICO. We first estimate the best, minimum and maximum present-day ocean input thermal driving in the respective region (see Appendix A2). Our best estimates for FRIS and the ASE are 0.53 and $1.65°\mathrm{C}$, respectively, and the minimum (FRIS: $0.13°\mathrm{C}$, ASE:$1.04°\mathrm{C}$) and maximum (FRIS: $0.84°\mathrm{C}$, ASE: $2.34°\mathrm{C}$) are taken from all values in Table A1. Those values are obtained by following the PICO procedure to average ocean conditions at depth over the continental shelf in front of the ice shelf cavity, which is a simplification that means that different water masses get mixed together and not only inflow water masses are considered (e.g. High Salinity Shelf Water which makes most of the inflow into the FRIS cavity would be at $0°\mathrm{C}$ thermal driving with respect to the surface melting point). Since we are mainly interested in the melt rates provided to the ice shelf, we focus here on obtaining correct melt rates as well as melt sensitivities.

Then we derive the sensitivity between ice melt and baseline temperatures, using an increase in 1 Kelvin. We test using a narrower or wider interval for the linearisation and find that the baseline temperature has a larger influence on the sensitivity than the temperature range over which it is linearised: for example, shifting the baseline temperature by 0.5 K gives a larger

https://doi.org/10.5194/tc-2022-105
Preprint. Discussion started: 31 May 2022

increase or decrease in the sensitivity than estimating the sensitivity over a temperature range of 0.5 or 2 K. We thus overall capture different ranges of the linearisation interval by using different input temperatures (best, min, max). Sensitivities are added as text fields in Fig. 2.

For FRIS, we find a sensitivity between 0.7 and 1.5 $\mathrm{ma}^{-1}\mathrm{K}^{-1}$ with the best estimate being 1.1 $\mathrm{ma}^{-1}\mathrm{K}^{-1}$. Jenkins (1991) find an increase from 0.6 ma^{-1} to 2.6 ma^{-1} for a warming by 0.6 K using plume theory, which implies a higher sensitivity of 3.3 for $\mathrm{ma}^{-1}\mathrm{K}^{-1}$ for FRIS. Hellmer et al. (2012) report that a switch from cold to warm conditions increases average melt rates from 0.2 to 4 ma^{-1} for a warming of 2 K, which implies also a higher sensitivity of 1.9 $\mathrm{ma}^{-1}\mathrm{K}^{-1}$. From Comeau et al. (Fig. 9d and S10, 2022) we roughly estimate a melt sensitivity of 3.5 $\mathrm{ma}^{-1}\mathrm{K}^{-1}$. The order of magnitude is in all cases comparable. We want to note here that currently no changes are observed in the ice streams in the Weddell Sea as have been reported for the ice streams in the ASE. Having the precisely correct sensitivity is hence less important for our study.

By comparison, the sensitivity for the ASE is higher (Fig. 2a). This might be due to the higher baseline temperatures and a larger slope of the ice shelf base (Jenkins et al., 2018). The sensitivity estimate based on the 'best' baseline temperature of 15 $\mathrm{ma}^{-1}\mathrm{K}^{-1}$ for Dotson Ice Shelf fits well with the estimate from Payne et al. (2007) for Pine Island Glacier Ice Shelf, which is 16 $\mathrm{ma}^{-1}\mathrm{K}^{-1}$. It is close to the initial sensitivity around 16 $\mathrm{ma}^{-1}\mathrm{K}^{-1}$ in Seroussi et al. (2017) for Thwaites Glacier Ice Shelf estimated from ocean simulations with an 0.5 K temperature increase, see Fig. S5 in the Supplement of Reese et al. (2020). The sensitivity in the coupled simulation of Seroussi et al. (2017) decreases during the simulation with a minimum value of 4.5 $\mathrm{ma}^{-1}\mathrm{K}^{-1}$, and a mean of 9 $\mathrm{ma}^{-1}\mathrm{K}^{-1}$, with the latter more in line with the minimum sensitivity estimate.

Using these target sensitivities (min, best, max for FRIS and ASE), PICO parameters can be optimized as presented in the following section.

3.3 Results: PICO parameter selection

We select PICO parameters such that the melt sensitivity is in line with estimates from the previous section and such that the underlying assumptions of PICO are met (similar to the approach in Reese et al., 2018a). In total, we optimize five pairs of parameters that span the range of different target sensitivities in FRIS and the ASE presented in the previous section. A summary of the results is given in Table 1.

We conduct a parameter sweep with PICO for different values for C and $\gamma_T^\star$, see Fig. 3. To have the melt rates calculated by PICO replicate present-day observations (in $\mathrm{Gt\,a}^{-1}$ from Adusumilli et al., 2020), we apply temperature corrections between -2 and 2 K to the underlying present-day temperatures from Schmidtko et al. (2014) in each basin. This is similar to the approach used by Jourdain et al. (see Section 4.4 in 2020). Temperature changes of this order of magnitude almost span the entire variation of ocean temperatures observed in the Southern Ocean and large temperature corrections could point to missing assumptions in the melt calculation. However, we are here interested in the ice sheet response, and for the ice sheet it is overall important to have the correct melt rates in present-day as well as the correct increase in melt rates with ocean temperature changes, which is achieved by this method.

Note that PICO generally shows a linear melt sensitivity, but we still make sure to optimize temperature corrections and melt sensitivity consistently by first calculating the temperature correction for all parameter pairs $(C, \gamma_T^\star)$ tested, and then selecting

https://doi.org/10.5194/tc-2022-105
Preprint. Discussion started: 31 May 2022

The Cryosphere Discussions

Table 1. Results of PICO parameter optimization. We optimize parameters for five combinations of sensitivity targets (selected from 'best', 'min', 'max' for FRIS and ASE). For each pair of target sensitivities we summarise the baseline thermal driving TD used for the linearisation to obtain the target sensitivity $\frac{dm}{dTD}^{target}$ for FRIS and ASE. Parameters are evaluated based on the match of modeled sensitivities $\frac{dm}{dTD}^{PICO}$ with target sensitivities. Then we give the optimized PICO parameters C and $\gamma_T^\star$ which are similar for all Antarctic ice shelves. For details see Sect. 3.2 and 3.3.

sensitivity targets	TD (°C)	$\frac{dm}{dTD}^{target}$ ($\mathrm{ma^{-1}K^{-1}}$)	$\frac{dm}{dTD}^{PICO}$ ($\mathrm{ma^{-1}K^{-1}}$)	C ($\mathrm{Svm^3kg^{-1}}$)	$\gamma_T^\star$ ($\times 10^{-5}\mathrm{ms^{-1}}$)
FRIS best	0.53	1.11	1.20	2.0	5.5
ASE best	1.65	15.04	15.25	2.0	5.5
FRIS min	0.13	0.68	0.73	1.0	4.0
ASE min	1.04	10.79	10.76	1.0	4.0
FRIS max	0.84	1.45	1.59	3.0	7.0
ASE max	2.34	19.91	19.49	3.0	7.0
FRIS max	0.84	1.45	1.43	3.0	4.0
ASE min	1.04	10.79	12.71	3.0	4.0
FRIS min	0.13	0.68	0.89	1.0	10.0
ASE max	2.34	19.91	19.04	1.0	10.0

the optimal parameter pair based on physical constraints on the corresponding melt rates and the resulting sensitivity estimates. With the parameter optimization, we thus obtain a set of two parameters $(C, \gamma_T^\star)$ and temperature corrections δT_b, for each basin $b \in 1, \ldots 19$ for each combination of target sensitivities.

We select the best parameters using four criteria: (1) melting (no freezing) occurs in the first box of PICO close to the grounding line, (2) melting in the first box is larger than in the second, (3) the melt sensitivity for FRIS is close to the target from Sect. 3.2, (4) the melt sensitivity in the ASE is close to the target from Sect. 3.2. Criteria (1) and (2) are analogous to the original parameter selection of PICO in Reese et al. (2018a). In the original selection, we also ensure that melt rates were comparable to observations in FRIS and the ASE. However, our aim here is to accurately capture the *sensitivity* of ice melt to temperature changes, as obtained by the new criteria (3) and (4). To ensure that present-day melt rates are consistent with observations, we apply the temperature corrections. See Tables S1 to S5 for the corresponding temperature corrections and comparison with observed melt rates for each parameter pair.

Table 1 shows that for all combinations of target sensitivities, the sensitivities modelled by PICO are generally in close agreement with the targets. In general, we find that higher sensitivities require higher parameter values. Sensitivities in the large-scale ice shelves such as FRIS are dominated by the overturning coefficient, which shows in the high value of C for high sensitivity targets in FRIS and low sensitivity targets in the Amundsen Sea. In the opposite case with high sensitivity target in the Amundsen Sea and a low target in FRIS, we find that for the smaller ice shelves the heat exchange coefficient $\gamma_T^\star$ is more important. In comparison with Reese et al. (2018a), we find overall higher parameter values: the value for C from the original

https://doi.org/10.5194/tc-2022-105
Preprint. Discussion started: 31 May 2022

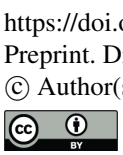

The Cryosphere
Discussions
Open Access
EGU

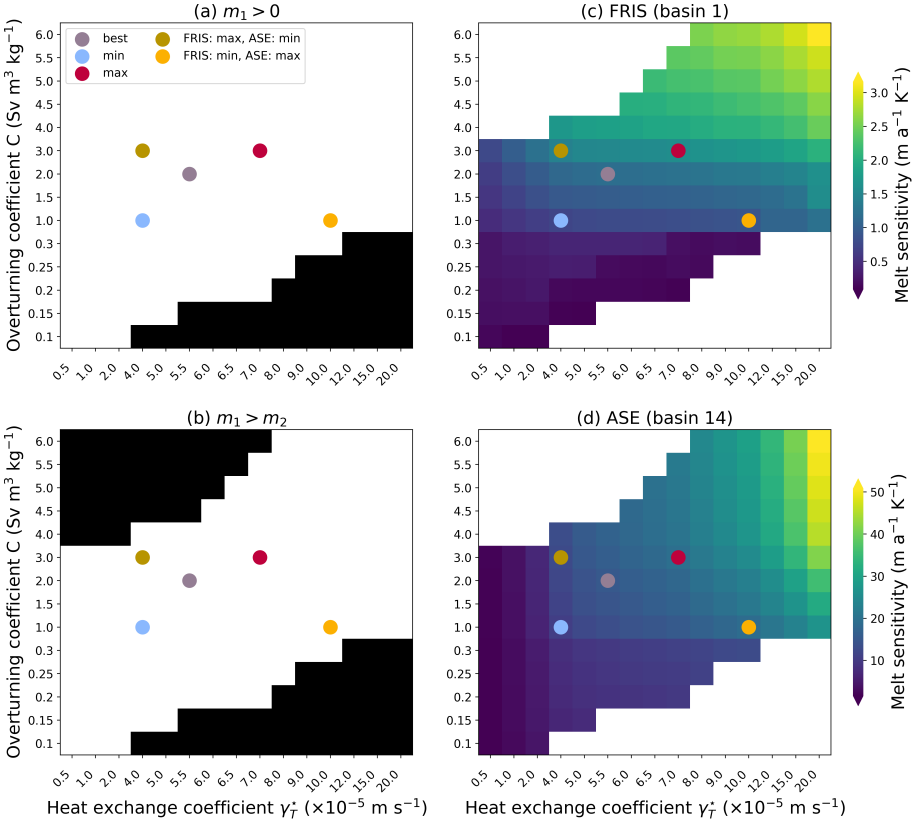

Figure 3. PICO parameter selection. Four targets are used for the optimisation of the heat exchange and overturning coefficients: (a) melting and not freezing in the first box close to the grounding line which is true in the white areas, (b) melt decreases away from the grounding line, i.e., melt rate in PICO box 1 is larger than in PICO box 2, which is true in the white colored areas (c) sensitivity of FRIS and (d) sensitivity of the ASE, both match estimates from Sect. 3.2. The latter two criteria are depending on the baseline temperature for the melt curve, which can yield best, min, max or mixed sensitivities (indicated by dots). Note that parameter spacing is not equal and melt sensitivities in (c) and (d) have a different scale ranging over the modelled sensitivities in PICO. The white boxes in (c) and (d) indicate regions where the criteria (a) and (b) fail.

235 tuning is now valid for a low sensitivity, while in all cases the value for the heat exchange is now higher. This is in line with a rather low sensitivity found in Reese et al. (2020).

In the PISM experiments presented in the rest of the manuscript, the 'best' fit parameters $C = 2\ \mathrm{Svm^3kg^{-1}}$ and $\gamma_T^\star = 5.5 \times 10^{-5}\ \mathrm{ms^{-1}}$ are used.

https://doi.org/10.5194/tc-2022-105
Preprint. Discussion started: 31 May 2022

4 Antarctic Ice Sheet simulations with PISM

In this section we describe the PISM simulations conducted using the newly optimised PICO parameters. We first describe the model and the experimental design, see Sect. 4.1 and 4.2, then the ensemble of historic simulations, see Sect. 4.3, and finally present results on the long-term evolution of Antarctica grounding lines under present-day climate conditions, see Sect. 4.4, and analyse their reversibility, see Sect. 4.5.

4.1 PISM

The Parallel Ice Sheet Model (PISM; https://www.pism.io; Bueler and Brown, 2009; Winkelmann et al., 2011) is an open-source ice dynamics model and is developed at the University of Alaska, Fairbanks, and the Potsdam Institute for Climate Impact Research.

PISM is thermo-mechanically coupled and employs a hybrid of the Shallow Shelf Approximation (SSA) and Shallow Ice Approximation (SIA) to model ice flow. Temperatures within PISM are determined based on an energy-conserving enthalpy scheme including a thin subglacial water layer and a thermal layer in the bedrock (Aschwanden et al., 2012). A power-law relationship is applied between SSA basal sliding velocities and basal shear stress with a Mohr–Coulomb criterion relating the yield stress to parameterized till material properties and the effective pressure of the overlaying ice on the saturated till (Bueler and van Pelt, 2015). Both, the grounding line and the calving front are simulated at subgrid scale in PISM and evolve according to the physical boundary conditions. Basal friction is linearly interpolated on a sub-grid scale around the grounding line (Feldmann et al., 2014). In order to improve the approximation of driving stress across the grounding line, the surface gradient is calculated using centered differences of the ice thickness across the grounding line. Sub-shelf melt rates are modelled using PICO and we use the set of optimal PICO parameters obtained with the new approach for the 'best' baseline temperatures (Sect. 3). In this study we conduct an equilibrium spin up, and as a result glacial isostatic rebound is switched off, because it would require a paleo spinup to correctly reproduce representative present-day uplift rates. We do not apply sub-shelf melt in partially floating grid cells and we only calve ice that extends beyond the present-day extent of the Antarctic ice sheet and ice shelves. Due to adaptive time-stepping and the employment of the SIA and SSA, PISM is computationally efficient and capable of simulating large ensembles on multi-millennial time-scales.

4.2 Experimental design and initialisation

The primary aim of this manuscript is to analyse the long-term evolution of Antarctic grounding lines under current climate conditions. To do this, we first require initial configurations that represent the Antarctic Ice Sheet under present-day climate conditions. We then run these initial states forward in time, and let them evolve under constant atmospheric and ocean conditions.

The strategy adopted to build initial present-day ice sheet configurations with PISM relies on spin-up. We test for uncertainties in model parameters by creating an ensemble of states and selecting a number of possible configurations that compare best

https://doi.org/10.5194/tc-2022-105
Preprint. Discussion started: 31 May 2022

to observations. For all ensemble members, we run historic simulations from 1850 to 2015 with the aim to reproduce current changes in ice sheet thickness.

To represent atmospheric and oceanic changes between 1850 to 2014 we use the historic forcing suggested by the Ice Sheet Model Intercomparison Project for CMIP6 (ISMIP6, Barthel et al., 2020; Seroussi et al., 2020), since no observations exist for that period in Antarctica. We apply the results from the Norwegian Earth System Model (NorESM; Bentsen et al., 2013), one of the ISMIP6-suggested climate models. The NorESM simulations do not provide a perfect representation of the past climate evolution, but it was found to have the smallest biases in the Southern Ocean and atmosphere (Barthel et al., 2020). Present-day ocean conditions are given by the data of Schmidtko et al. (2014), which are adjusted using the basin-wide temperature corrections from the PICO parameter optimisation presented in Sect. 3.3, and atmospheric surface mass balance and surface temperatures are used from RACMOv2.3 (1995 to 2014 averages, van Wessem et al., 2018). These datasets are used for present-day climate, and anomalies are applied from the NorESM-1 output, following ISMIP6. This approach captures transient changes in the atmosphere or ocean while linearly correcting biases. Ocean and atmosphere climate conditions for the equilibrium state in 1850 were obtained as follows: we first generate a timeseries of atmosphere and ocean anomalies from the modelled historic evolution that pass through zero anomalies between 1995 and 2014. We then add these anomalies to the present-day climatologies for the atmosphere and ocean which make sure that our forcing timeseries passes through the present-day dataset in the period between 1995 and 2014. Finally we take the average over the first 30 years of the respective timeseries to arrive at historic conditions. Note that the atmospheric forcing as provided by ISMIP6 starts in 1950 and we keep it constant at the 1950 to 1980 average between 1850 and 1950.

Using these boundary conditions, the initial configurations are obtained as follows. Starting from BedMachine ice thickness and topography (Morlighem et al., 2020), PISM is run for 400,000 years with constant geometry to obtain a thermodynamic equilibrium using a 16 km spatial grid resolution. After this, an ensemble of simulations with varying model parameters is run for several thousand years towards dynamic equilibrium on 8 km horizontal resolution using historic climate conditions around 1850. We thus make the conservative assumption that the ice sheet was close to equilibrium in 1850 which was likely not the case. Our assumption means that any tipping point that might be crossed due to climate changes prior to 1850 cannot be discovered with our methodology. However, starting from a state that is close to equilibrium in 1850 allows us to directly attribute any committed changes under present-day climate to the historic forcing.

The simulations employ 121 vertical layers with a quadratic spacing from 13 m at the ice shelf base to 100 m towards the surface. We vary parameters related to basal sliding and ice flow, in particular we vary the SIA enhancement factor ($E_{SIA} \in \{1.5, 2\}$; Winkelmann et al., 2011), the till effective overburden fraction ($\delta \in \{1, 1.5, 2, 2.5, 3\}\%$; Bueler and van Pelt, 2015), the decay rate of till water content ($C_d \in \{7, 10\}\ \mathrm{mm\,a^{-1}}$; Bueler and van Pelt, 2015), and the piecewise linear, parameterised till friction angle (smallest values $\Phi_{min} \in \{20, 24\}^\circ$ are used for topography below -700m, largest values $\Phi_{max} \in \{30, 50\}^\circ$ are used for topography above 500 or 1000m, respectively; Martin et al., 2011). This yields 40 ensemble members to start with.

After 5000 years of model simulation, we select five ensemble members that compare best to present-day observations of ice geometry and speed (Morlighem et al., 2020; Mouginot et al., 2019) for the entire ice sheet, and for each of the Amundsen, Ross and Weddell sea sectors. This makes 16 members in total due to overlaps between the best members for the different regions.

https://doi.org/10.5194/tc-2022-105
Preprint. Discussion started: 31 May 2022


The Cryosphere Discussions
Open Access
EGU

Table 2. PISM parameters used for the 9 ensemble members. Runs are sorted starting with the best scores shown in Fig. B1.

	$\delta(\%)$	$\phi_{min}(^\circ)$	$\phi_{max}(^\circ)$	$h_{max}(\mathrm{m})$	E_{SIA}	$C_d(\mathrm{mm/a})$
ANT1	2.0	24.0	30.0	500.0	2.0	10
ANT2	2.0	24.0	30.0	500.0	2.0	7
ANT3	2.0	20.0	50.0	1000.0	2.0	10
ANT4	2.5	20.0	50.0	1000.0	2.0	10
ANT5	2.5	24.0	30.0	500.0	2.0	10
ANT6	1.5	24.0	30.0	500.0	2.0	7
ANT7	1.5	20.0	50.0	1000.0	1.5	7
ANT8	1.0	24.0	30.0	500.0	2.0	7
ANT9	1.0	20.0	50.0	1000.0	2.0	7

We assess the ensemble members using a scoring method (Albrecht et al., 2020; Reese et al., 2020) that tests the root-mean-square deviation to present-day ice thickness, ice-stream velocities, as well as deviations in grounded and floating area, and the average distance to the observed grounding line position. We lay a specific focus on the Amundsen region, Filchner-Ronne and Ross ice shelves by additionally evaluating each indicator for these drainage basins individually. The selected 16 ensemble members are then continued until they reach 25,000 years. From these, seven members were discarded due to ongoing advance in the large ice shelves or collapse of the West Antarctic Ice Sheet in the control simulations.

After the 25,000 year equilibrium spin up we then use the remaining ensemble of nine initial states, summarised in Table 2, to run historical simulations from 1850 to 2015 which are forced by changes in the ocean and atmosphere as described above. The corresponding changes in ocean temperature and salinity input for PICO are shown in Fig. S1. These runs are evaluated again, now including also a comparison with present-day mass losses in the metric. The scoring of the present-day states is shown in Fig. B1 and the best run is used for the experiments in Urruty et al. (subm.).

To understand the long-term evolution of Antarctic grounding lines, all these nine runs are then continued under present-day climate conditions for 10,000 years (in total we run thus $25,000 + (2015 - 1850) + 10,000$ years). To test the effect of uncertainties in present-day ocean temperatures, we add two simulations for one of the best-scoring initial states (second in Fig. B1, ANT2) with a stronger increase in ocean temperatures by $+0.1$ and $+0.3$ K uniformly for all Antarctic ice shelves. To this aim we add the uniform temperature increase in the long-term evolution simulations after 2015. We run control simulations with constant 1850 climate conditions parallel to all simulations to exclude that any remaining trends in the initial state might influence the results, see Fig. B2.

To test for reversibility, we revert the climate forcing back to the 1850-conditions in simulations in which we find large-scale retreat during these 10,000 years. We then extend those simulations for another 20,000 years with constant historic climate.

https://doi.org/10.5194/tc-2022-105
Preprint. Discussion started: 31 May 2022

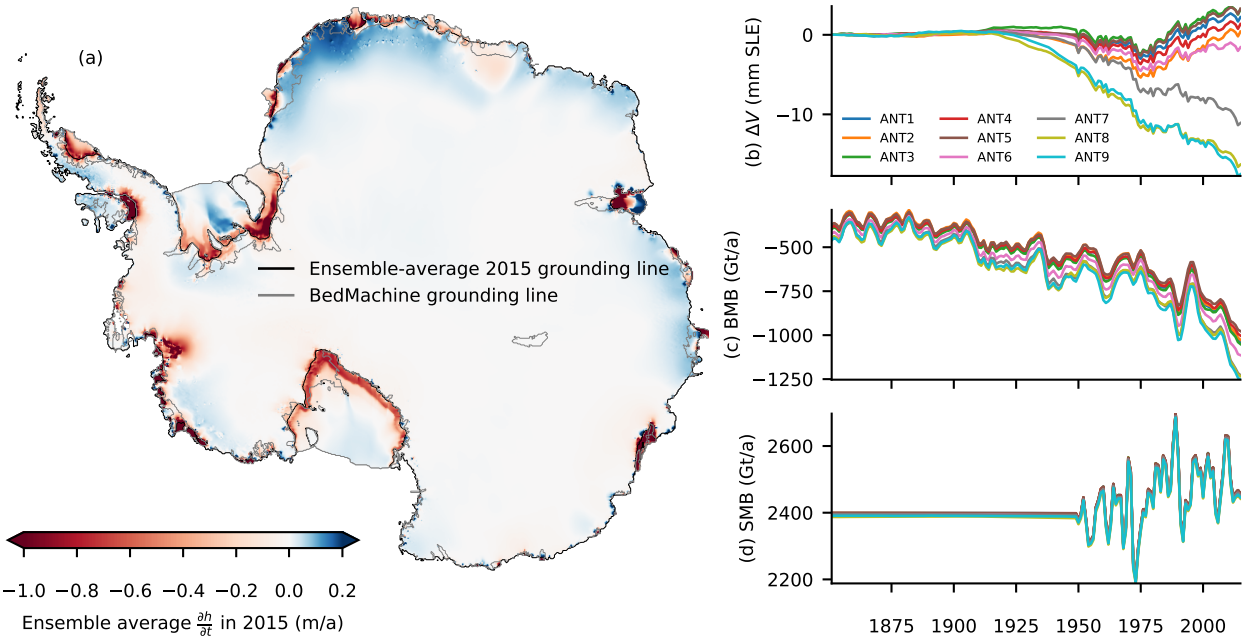

Figure 4. Historic simulations from 1850 to 2015 and present-day ice sheet configurations. Shown are (a) ensemble-average rates of ice thickness changes in 2015 (relative to control) with average grounding line position, and evolution of (b) the sea-level relevant ice volume (in millimetres sea-level equivalent, mm SLE), (c) basal mass balance, and (d) surface mass balance (both in gigatons per year).

Table 3. Modelled mass loss between 1850 and 2015, between 1992 and 2015, and drift in control run between 1850 and 2015 in mm SLE for the 9 ensemble members. This can be compared to observed mass loss of 7.6 ± 3.9 mm SLE between 1992 and 2017.

	$\Delta V_{1850-2015}$	$\Delta V_{1992-2015}$	Drift $\Delta V_{CTRL,1850-2015}$
ANT1	-2.20	-2.59	5.07
ANT2	-0.41	-3.50	3.31
ANT3	-3.18	-2.66	4.93
ANT4	-1.34	-2.83	4.36
ANT5	-3.27	-2.99	4.52
ANT6	1.59	-1.31	3.99
ANT7	11.13	3.35	2.18
ANT8	16.33	3.53	7.93
ANT9	17.55	4.53	4.29

Mass loss is given relative to control simulations.

https://doi.org/10.5194/tc-2022-105
Preprint. Discussion started: 31 May 2022

4.3 Results: Historic simulations and present-day ice sheet configurations

Starting from quasi-equilibrium states and 1850 climate conditions, we run all nine members of the ensemble of initial configurations from 1850 to 2015 with changes in the ocean as well as the atmosphere as described in Sect. 4.2. Figure 4 presents the results at the end of these historical simulations (2015) and shows that in 2015, the rates of ice thickness change averaged over all ensemble members generally resembles the observed pattern, see for example Smith et al. (2020). In general, thinning occurs in accordance with observations in the Amundsen and Bellingshausen Sea sectors, along the Antarctic Peninsula and for Totten and Moscow-University ice shelves. Also in line with observations thickening due to increased snowfall is found in the interior of the ice sheet. In contrast to observations, the simulations also show thinning in and upstream of Ross, Filchner-Ronne and Amery ice shelves and in some places along Dronning Maud Land because of ocean temperature increases in these areas. This might not be representative of actual ongoing changes since coarse-resolution climate models cannot fully resolve the important processes on the continental shelf. This discrepancy from observations must be taken into account when interpreting the results of the long-term simulations.

While the pattern of thinning and thickening is overall comparable with observations, the thinning rates in the ASE sector are rather low and do not extend as far inland as in observations. As a result, simulated integrated mass losses for present-day (see Table 3) are generally at the lower end of observations of 7.6 ± 3.9 mm SLE between 1992 and 2017 (Shepherd et al., 2018). Six of nine ensemble members shows no mass loss or even mass gain in that period, see also Table 3. There are several possible reasons for this: snowfall increases might be too high, the effect of calving and damage is missing in the simulations, changes in the ocean forcing or translation to basal melting might be too weak, we apply no melt in partially floating grid cells at the grounding line. Higher mass loss might be expected with higher resolution < 8 km, also particularly mass loss at Pine Island Glacier (PIG) is lower than in observations, potentially due to the rather coarse resolution or its grounding lines being downstream of the observed position. Overall, this suggests that our results for the long-term evolution in the next section overestimate changes in the cold cavity ice shelves like Ross and FRIS and underestimate changes in the ASE.

We find that the magnitude of mass loss depends strongly on sliding parameters. This, as well as the choice of the sliding law, has been found also in previous studies (Brondex et al., 2019). Higher mass losses occur for lower values of δ which is a parameter defining the fraction of the effective pressure on the till to the ice overburden pressure for fully saturated till. Lower values of this parameter yield more slippery bed conditions in particular for ice streams, in line with a stronger response to buttressing loss through increases ocean-driven sub-shelf melting. However, those simulations tend to have the grounding line of Thwaites Glacier upstream of present-day (see Fig. S2).

All runs show grounding lines for Filchner-Ronne and Amery ice shelves that are extended seaward of observations. This is maybe an artefact of creating an equilibrium state at 1850 climate conditions, a problem with the initial climate used or with the coarse sampling of water masses in PICO. Furthermore, runs show a retreated grounding line in the Siple Coast of Ross which is a problem encountered often in spin-up as this region is close to flotation.

Generally, sub-shelf melt increases from 1850 onward to values between 900 to 1200 Gta^{-1} in 2015, comparable to observations ranging between 1173.1 ± 148.5 Gta^{-1} in 1994, $1{,}570 \pm 140$ Gta^{-1} in 2009 and $1{,}160 \pm 150$ Gta^{-1} in 2018 (Adusumilli

https://doi.org/10.5194/tc-2022-105
Preprint. Discussion started: 31 May 2022

Table 4. Committed mass loss after 10,000 years (in m SLE).

	$\Delta V_{12,015-2015}(\mathrm{m\,SLE})$
ANT1	-0.76
ANT2	-0.81
ANT3	-0.77
ANT4	-0.69
ANT5	-0.59
ANT6	-0.89
ANT7	-2.84
ANT8	-2.48
ANT9	-2.23
ANT2 ΔTD = 0.1 K	-1.49
ANT2 ΔTD = 0.3 K	-4.15

et al., 2020). Differences between ensemble members occur due to different ice shelf extents in the initial states. Our historic simulations do not replicate the particularly high melt fluxes in 2009 which may be a reason why overall mass losses are at the lower end of observations.

Surface mass balance varies only from 1950 onward since no data were available beforehand and extended constantly back in time. It is more similar for all ensemble members since the maximum ice extent is pre-defined based on BedMachine Antarctica and the integrated surface mass balance is hence similar for all members.

We note that the control simulations do yet not reach a full equilibrium, even after 25,000 years in their 1850 initial configurations, see Fig. B2. We continue the control runs parallel to the historic simulations and for further 10,000 years. During the historical simulations (years 1850 to 2015) the drift is 2-8 mm SLE (see Tab. 3). Only runs that remain close to their 1850 configuration are used here. Figure B2 shows that grounding lines move only a little for the ensemble presented and that rates of volume change monotonically decrease towards zero.

4.4 Results: Long-term grounding line evolution under present-day climate conditions

We investigate the long-term evolution of present-day Antarctic grounding lines by keeping the present-day climatology constant following the historic simulation and letting the ice sheet state evolve towards a new equilibrium for 10,000 years. We then investigate if the grounding lines remain close to their currently observed position or if they retreat substantially.

Figure 5 shows that the grounding lines of the present-day configurations retreat in some simulations substantially in the marine regions of West Antarctica. Overall, mass loss ranges between 60 cm and more than 4 m SLE, which is lost over 10,000 years (see Table 4). Note that most states are still losing ice at the end of the simulation time, and thus grounding lines might not have converged fully to a new stable steady state position.

https://doi.org/10.5194/tc-2022-105
Preprint. Discussion started: 31 May 2022

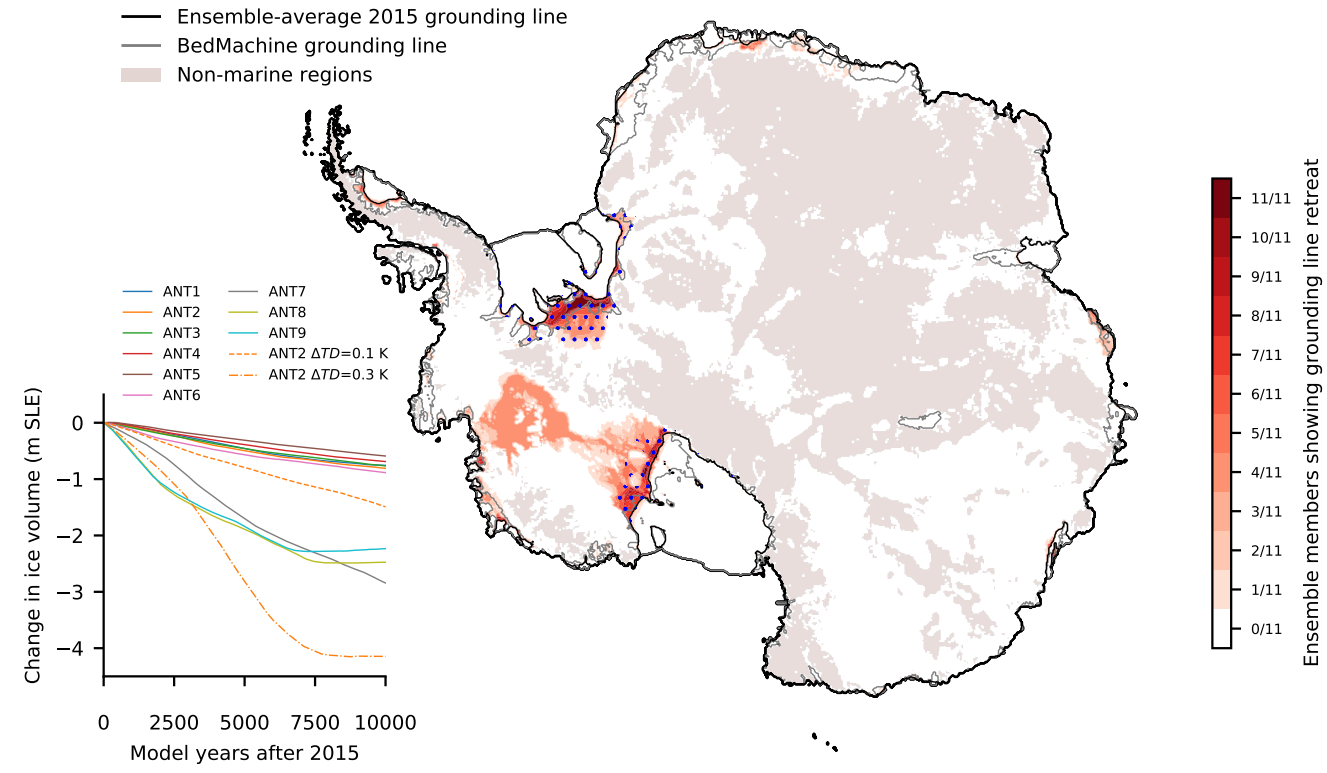

Figure 5. Long-term evolution of present-day Antarctic grounding lines under constant present-day climate conditions. Starting in present-day after the historic forcing from 1850 to 2015, simulations are continued with constant present-day climate for 10,000 years. Red colors show regions over which the grounding line retreats. The darker the red, the more simulations show grounding line retreat over the respective region in the different simulations corresponding to variations in basal sliding and ice flow parameters (retreat is plotted in comparison to a control simulation). Black contour shows ensemble-average initial grounding line position in 2015. Inset shows the evolution of sea-level relevant ice volume for all ensemble members (m SLE, metres sea-level equivalent). Dots on retreat areas indicate regions in which present-day modelled thinning deviates from observations (namely for FRIS and Ross ice shelves). Light brown indicates bedrock above sea level, white areas indicate bedrock below sea level. Note that retreat occurs only in marine regions which have bedrock below sea level.

Substantial retreat and the associated loss of large parts of the marine basins is found in the ASE sector, upstream of Thwaites Glacier. This occurs for ensemble members with more slippery bed conditions or higher ocean temperatures. Grounding lines and ice thickness changes are shown in Fig. S3. Ensemble members that show this widespread collapse are ANT7, ANT8

https://doi.org/10.5194/tc-2022-105
Preprint. Discussion started: 31 May 2022

and ANT9, which have lower δ parameter values. Also, the run testing a $+0.3$ K higher ocean forcing for a non-collapsing state ANT2 with more rigid bed conditions shows collapse. Note that the more slippery ensemble members have present-day grounding lines upstream of their present-day locations for Thwaites Glacier and, at the same time, are better at reproducing present-day observed mass losses.

The experiments with increased ocean forcing were conducted using one of the initial states that best replicated observations. The state itself shows limited retreat of the the grounding lines over the 10,000 years. However, smaller tipping points might be crossed, as discussed in the case of Dotson and Crosson ice shelves in the companion paper (Urruty et al., subm.). We find that for +0.1 K higher ocean temperatures in present-day substantial retreat occurs in FRIS and Ross Ice Shelf, but not in the Amundsen Sea. For +0.3 K higher present-day ocean temperatures, WAIS collapses from both directions, the Amundsen and the Ross Seas. This indicates that large-scale retreat of all marine regions in West Antarctica is very sensitive to small changes in the ocean temperatures.

No retreat of Pine Island Glacier upstream of its present-day position is found. However, as discussed in the previous section, Pine Island Glacier's grounding line is too far downstream of present-day in all ensemble members, and modelled present-day thinning rates are too low in comparison with current observations. We think that a more detailed high-resolution modelling study would be required to analyse the committed evolution of Pine Island Glacier. We find some retreat in Smith, Kohler and Pope glaciers, which does, however, not extend very far upstream of the present-day grounding line positions.

We find that all ensemble members retreat in the regions that span between the Robin subglacial basin and the ice rumples in Ronne Ice Shelf that was grounded in the initial states although it is floating in observations. However, only about half of the runs continue beyond present-day grounding line positions. As we discussed in the previous section, this region shows thinning after the historic simulation which is not in line with observations. This hints at an issue with the historic ocean forcing in this area, which could be the general circulation model simulation, but also that PICO does not modify water masses on their way into the cavity and translates all changes on the continental shelf in front of the cavity directly into changes in the cavity.

Grounding lines retreat for almost all members of the ensemble in the Siple Coast of Ross Ice Shelf. Simulations with more slippery bed conditions show stronger retreat. Similar to FRIS, the historic runs show thinning in this region which is not compatible with observations. Further work is required for both ice shelves to understand current climate forcing and committed retreat.

In all other regions of Antarctica we find only small retreat of grounding lines.

4.5 Results: Reversibility of large-scale retreat

To test for the reversibility of large-scale retreat found in four ensemble members in the previous section, we reverse climate forcing back to pre-industrial, 1850 conditions and extend the four simulations that show large-scale retreat for another 20,000 years. Figure 6 shows that rates of ice thickness change in the end of the reversibility runs are small enough to consider the grounding lines close to steady state. We find that retreat in Thwaites Glacier shows overall no reversibility with the reversed grounding line usually close to the collapsed one in all four simulations. In the ANT7 and ANT2$+0.3$ K simulations, the grounding line shows some advance, but halts substantially upstream from its current position. In contrast, FRIS shows a clear

https://doi.org/10.5194/tc-2022-105
Preprint. Discussion started: 31 May 2022

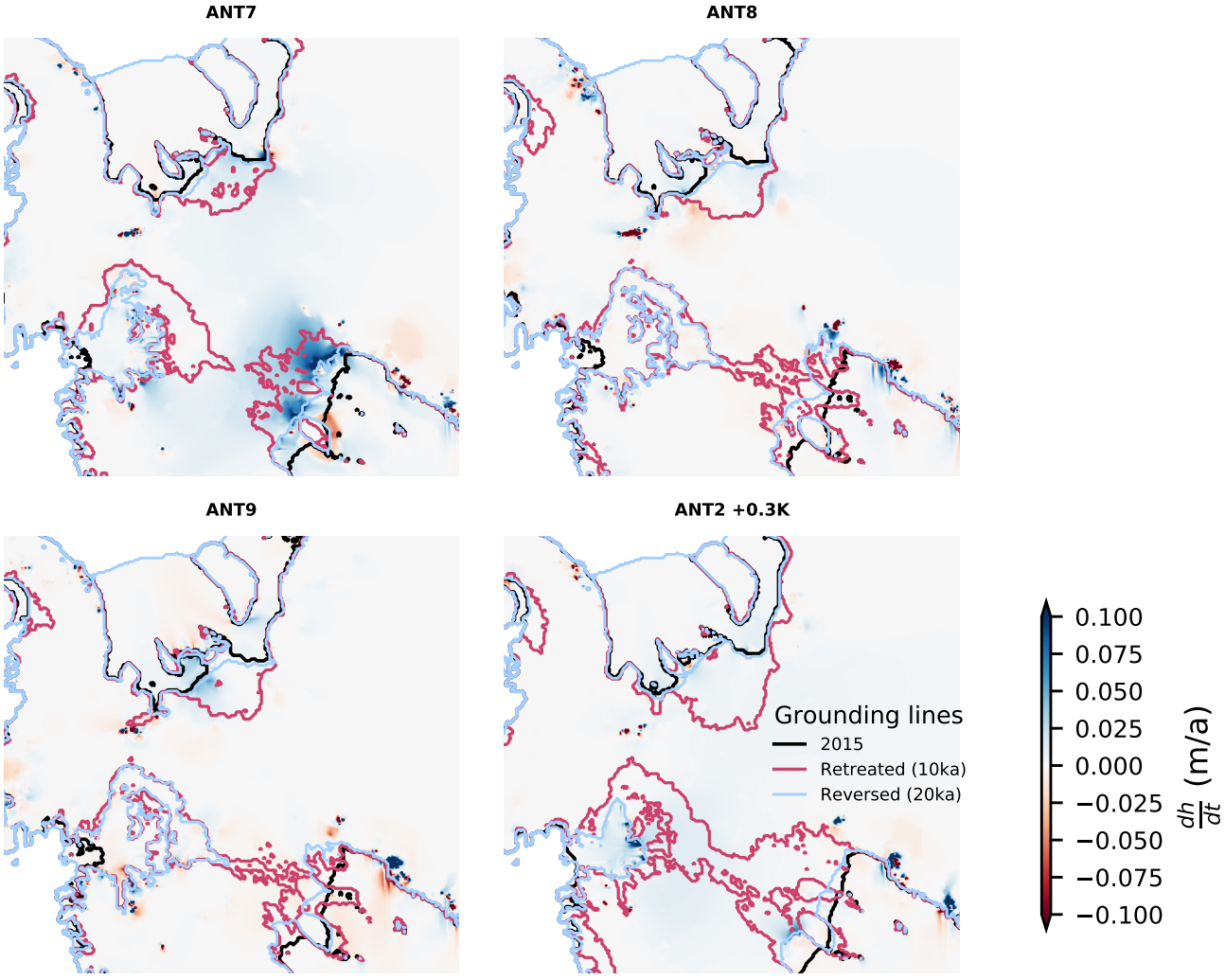

Figure 6. Reversibility experiments of large-scale retreat in West Antarctica. Four present-day configurations, with their 2015 grounding lines shown in black, show large-scale retreat under constant present-day climate (red lines show grounding line positions after 10,000 years), see also Fig. 5. When reversing the climate to historic conditions for 20,000 years, the grounding lines evolve to the positions shown in blue. The spatial map shows the rate of ice thickness change after the 20,000 years of reversal.

415 reversibility, with the grounding line advance to almost its present-day or historic position in the initial configurations. The Siple Coast in Ross Ice Shelf shows also reversibility in all four cases with the grounding line reaching a position slightly upstream of the modelled present-day location.

https://doi.org/10.5194/tc-2022-105
Preprint. Discussion started: 31 May 2022

5 Discussion

In the following, we discuss the optimization of PICO parameters and the PISM experiments. Based on these, we then draw conclusions on the potential states of Antarctic grounding lines discussed in Sect. 2.

5.1 PICO parameter selection

In this paper we have selected PICO parameters such that the sensitivity in FRIS and for the ASE ice shelves matches with independent estimates. This approach yields different parameters than previous studies (Reese et al., 2018a, 2020), but also than a recent study (with $\gamma_T^\star = 0.41 \times 10^{-5}\ \mathrm{ms}^{-1}$ and $C = 15.1\ \mathrm{Sv\,m\,kg}^{-1}$; Burgard et al., 2022) which optimized parameters to match with model simulations of NEMO (Nucleus for European Modelling of the Ocean) under present-day conditions. The earlier studies only used present-day melt rates as targets, not the sensitivity of melt rates which is arguably more important for perturbation experiments or projections. While the NEMO simulations did include variability in the ocean input, one reason for the differences in the parameters could be that the NEMO simulations did not include a similarly strong increase in melting of FRIS, which we use here explicitly for parameter optimization. Furthermore, here we concentrate on those two regions which classify as 'warm and small cavities' and 'as cold and large cavities', respectively, while Burgard et al. (2022) optimises parameters for all major ice shelves around Antarctica. Our parameters might hence not be suited for other ice shelves, in particular ice shelves in different regimes, e.g., 'small and cold cavities'. Note that these type of ice shelves might however not contribute substantially to sea-level in the future.

We conclude that the parameter selection for PICO should be adopted to the aim of the study in which they are applied. Since in our study we find most changes for the ASE sector and the large Filchner-Ronne and Ross ice shelves, we think that our parameter selection procedure with particular focus on these regions is appropriate. The way the parameters are selected, by linearising between present-day ocean temperatures and $+1$ K increased conditions, makes this method also applicable for conducting sea-level projections. As a next step, it would be interesting to test the effect of the uncertainty in the parameters, including uncertainties in the temperature corrections, on the evolution of grounding lines under constant present-day climate conditions, which was besides the aim of this work.

5.2 PISM experiments

Here we use a suite of PISM simulations that apply changes from 1850 to 2015 and then keep the present-day climate constant for 10,000 years to address the question of committed retreat under present-day climate conditions. In simulations that show large-scale retreat we reverse the forcing to 1850 conditions to test for reversibility of the grounding lines.

One caveat of the applied methodology is that we rely on the historic forcing by the general circulation model NorESM (Bentsen et al., 2013), which was selected by ISMIP6 due to its best performance around Antarctica (Barthel et al., 2020), but might represent trends in the atmosphere and ocean in some places incorrectly. In particular, currently no ice mass losses are observed in the Weddell and Ross Seas, however, we find thinning in these regions through the historic model simulations. In addition to the impact of the forcing from NorESM, the assumption of PICO, that ocean conditions on the continental shelf are

https://doi.org/10.5194/tc-2022-105
Preprint. Discussion started: 31 May 2022

directly translated into the ice shelf cavity, could introduce uncertainties. The committed specific patterns of retreat simulated in these regions must be interpreted with caution. Whether Ross and FRIS could become substantial contributors to sea-level rise in the future, or show tipping behaviour in the ocean (Hellmer et al., 2017; Naughten et al., 2021), is an active field of research. Understanding the committed evolution of both systems at present and under future warming in a coupled configuration would hence be of great interest.

On the other hand, our simulations have a tendency to underestimate present-day mass loss in the ASE sector. This might be explained by ocean forcing that is too weak in comparison to present day, but also other factors, like the horizontal resolution of 8 km in the model simulations. Generally ocean forcing in the Amundsen Sea is a complicated process (Jenkins et al., 2016; Holland et al., 2019) and more work is needed to understand its effect on the stability regime. We keep present-day climate conditions constant, but substantial decadal variability is observed in particular in the Amundsen and Bellingshausen Seas (Jenkins et al., 2018), which is known to influence numerical results (Hoffman et al., 2019).

While we find that ice sheet states with more rigid bed do not show committed WAIS collapse under present-day forcing, an increase in ocean temperatures by $+0.3$ K already changes that result. Similarly, we find retreat into marine basins upstream of Ross and FRIS to be sensitive to small variations in ocean temperatures. This indicates that only small changes in ocean conditions can have a huge effect on the long-term committed retreat. Improved data of the present-day forcing, and its variability, would be required to further investigate the commitment of WAIS collapse.

We here used an ensemble approach to better understand the influence of ice sheet model parameters on the sensitivity of present-day Antarctic grounding lines. Due to computational constraints, we could not explore the full parameter space. In particular, an important mitigating factor for MISI are gravity-induced sea-level changes at the grounding line (Gomez et al., 2010) as well as glacial isostatic rebound (Gomez et al., 2015). These feedbacks make grounding lines less prone to instability. For consistency with the two other models in the companion paper, those feedbacks are not accounted for in the PISM experiments. Also for that reason, we do not apply calving or adjustments to the surface mass balance to surface elevation changes. Note that these modelling choices make it possible to analyse the existence of MISI independently from the above mentioned positive or negative feedback mechanisms. Feedback mechanisms that are included in the simulations are thermomechanical feedbacks between sliding, saturation of the till and friction since we let the ice enthalphy and basal till water content evolve in the simulations. Furthermore, calving could influence the stability regime substantially (Haseloff and Sergienko, 2018). The way melting is applied at partially floating grid cells is known to influence the results (Seroussi and Morlighem, 2018), and we do thus not apply melting in partially floating cells here. A study with higher resolution of individual regions could help to understand the effect of potentially prohibiting melting over important regions close to the grounding line.

We start the historic simulations from an equilibrium state in 1850 which does not include the paleoclimate history of the Antarctic Ice Sheet. This means that any grounding line retreat that was committed before 1850 cannot be considered in this analysis. However, this approach makes it possible for us to perform a clearly defined analysis of the effect of the recent ice sheet history on its committed grounding line evolution. In their model simulation of the evolution of the Antarctic Ice Sheet since the last interglacial, Golledge et al. (2021) find the WAIS to retreat under current climate conditions. Their

https://doi.org/10.5194/tc-2022-105
Preprint. Discussion started: 31 May 2022

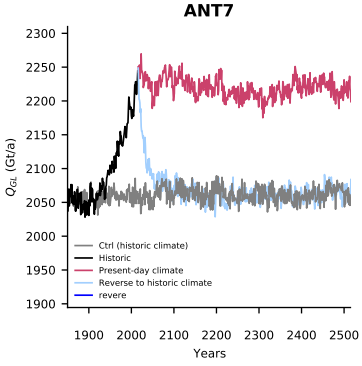

Figure 7. Example for reversibility in 2015. The simulation ANT7 shows large-scale WAIS retreat and an irreversible collapse of Thwaites Glacier under constant present-day climate conditions (grounding line flux shown in red), see Fig. 6. However, reversing the ocean and atmosphere back to 1850 conditions after 2015 allows the grounding line flux (light blue line) to reverse to the pre-industrial control (grey line) and prevents the collapse. We here show grounding line flux evolution over 500 years as done in Urruty et al. (subm.).

simulation includes glacial isostatic adjustment and calving, and is hence complementary to our approach. They do not test for irreversibility. It would be interesting, as a next step, to analyse the effect of the Antarctic Ice Sheet trajectory through the glacial cycles and deglaciation on the currently committed grounding line retreat and reversibility of retreat in more detail.

5.3 Potential states of Antarctic grounding lines

In Section 2 we discuss a classification of current Antarctic grounding lines with respect to MISI. We argue that four different grounding line states are possible: MISI exists and neither the critical parameter not the critical system state has been crossed (1, 'no instability') , MISI exists and the critical parameter has been crossed but not the critical system state (2, 'committed instability'), MISI exists and both, the critical system state and the critical parameter haven been crossed and the grounding line is engaged in an irreversible retreat (3, 'ongoing instability'), no MISI exists and all perturbations are reversible (4, 'no MISI').

Our reversibility experiments show that MISI exists for Thwaites Glacier, which is in line with previous findings for the ASE (Feldmann and Levermann, 2015) and excludes case (4). The experiments further show that grounding lines in Filchner-Ronne and Ross ice shelves are reversible, indicating them to be in state (4). This is in line with a modelling study finding a stable grounding line position on a retrograde sloping bed (Gudmundsson et al., 2012). This grounding line is buttressed (Gudmundsson, 2013) and grounding lines in Filchner-Ronne and Ross ice shelves were reported to show even stronger buttressing (Reese et al., 2018b). Also, theoretical work by Pegler (2018) and Haseloff and Sergienko (2018) did show that strong buttressing can suppress MISI. In our experiments we allow the ice shelves to regrow to their current extent. Haseloff and Sergienko (2018) showed that in the presence of buttressing, also the calving law influences the stability regime of grounding lines, and the implication of the calving law on the reversibility of Antarctic grounding lines should be explored further.

https://doi.org/10.5194/tc-2022-105
Preprint. Discussion started: 31 May 2022

That the 'overshoot' state (2) indeed exists for Antarctic grounding lines becomes clear from our experiments: we test one state that shows a long-term committed collapse in Thwaites Glacier, i.e., that could be in state (2) or (3), and reverse the forcing after the historic simulation until 2015 back to the 1850 climate conditions. This run shows reversibility (see Fig. 7). This state is hence indeed a case (2) state and the committed collapse can still be reversed in present-day. This is further underlined by running the perturbation experiments from Urruty et al. (subm.) in which we find no indication of MISI-driven retreat in the 2015 geometry, see Fig. S4. Other grounding lines show no large-scale retreat in our experiments. They are thus neither in state (2) nor (3) according to our simulations. If they are in state (1) or (4) cannot be concluded from our runs and more work would be needed to understand their potential for irreversible retreat. Overall, our results underline that observations of grounding line retreat cannot be interpreted as indications of irreversible retreat or collapse. Instead, dedicated numerical experiments are required to understand the underlying stability regime.

We want to note that our experiments in this paper do not directly test for the onset of MISI, but if the final retreat over large marine basins is reversible. Furthermore, since there is still a small drift in our simulations after 10,000 years, we did not fully identify the underlying stable steady state grounding line position. Further retreat is possible, and also those simulations that show no collapse could theoretically still show retreat and collapse after year 12,000. All results are hence given with reference to this time frame, but they allow us to analyse the tendency of the evolution of the system over a rather long period of time. Similar caveats apply for the re-advance simulations, which we ran over 20,000 years to reduce drift in the final states. In addition, our experiments focus on reversibility of large-scale retreat. Smaller tipping points might occur and be not distinguishable in the large-scale picture, see Rosier et al. (2021).

Our classification of Antarctic grounding lines (Sect. 2) is based on the assumption that steady state positions exist. Since ice dynamics is also influenced by thermodynamics, also oscillatory or limit cycle behaviour is possible. In this case the system would not settle on one stable steady state if run forward under constant conditions, but on a closed, oscillatory attractor (e.g., Feldmann and Levermann, 2017). However, a previous study that includes thermodynamics (Garbe et al., 2020) generally showed hysteresis behaviour for Antarctica on a broad scale, so we think that making this assumption is appropriate here. Similarly, other previous studies assessing the long-term (thousands to millions of years) hysteresis behaviour of the Antarctic Ice Sheet also show stable steady state behaviour, with cycle behaviour only induced by (cyclic) insolation forcing (e.g., Pollard and DeConto, 2005; Langebroek et al., 2009). This is also underlined by our control run experiments which show convergence of their ice volume towards steady states rather than large scale cyclic behaviour. Other feedbacks and processes than MISI might influence the stability regime of grounding lines, e.g., bedrock uplift and the melt-elevation feedback can lead to cyclic behaviour (Zeitz et al., 2021). We here exclude those feedbacks and only focus on MISI.

The timescales over which the WAIS collapses in our runs, are thousands of years. This timescale is similar to other studies that analyse tipping processes (Garbe et al., 2020; Rosier et al., 2021; Feldmann and Levermann, 2015; Mengel and Levermann, 2014). However, stronger forcing can increase the rates of mass loss substantially and shorten time scales. For example, following a complete removal of ice shelves, the WAIS was found to collapse within a few centuries (Sun et al., 2020). Also, the volume of committed ice loss we find is similar to previous studies. For example, Golledge et al. (2021) suggest a committed loss of up to 4 m SLE.

https://doi.org/10.5194/tc-2022-105
Preprint. Discussion started: 31 May 2022

6 Conclusions

In this manuscript we aim to understand the current state of Antarctic grounding lines by analysing their underlying steady states and the reversibility of large-scale transitions if they occur. Since a change in sub-shelf melt rates is thought to be a major trigger for grounding line retreat in Antarctica, we present a new parameter optimisation approach for the melt rate parameterisation PICO. This approach ensures that the sensitivity of melt rates to ocean temperature changes is in accordance with observations or high-resolution ocean simulations. This makes the parameters also suitable for sea-level projections. Using an ensemble of numerical simulations with PISM, we analyse the evolution of Antarctic grounding lines under present-day climate conditions. We find that for some possible representations in our ensemble, current climate conditions can force a retreat of Thwaites Glacier in the ASE sector which eventually results in an irreversible collapse. Note that this is not contradictory to the finding in the companion paper that grounding lines in Antarctica are currently not engaged in MISI (Urruty et al., subm.): grounding lines can be in an 'overshoot' state or state of 'committed instability' since grounding lines adjust to external forcing over long timescales of centuries to millennia. In this state they are not engaged in a MISI yet and their retreat is still reversible, but they might evolve towards an instability if climate conditions are kept constant. Our experiments show that for some ensemble members, Thwaites Glacier is in such a state. Furthermore, we find that large-scale retreat of the grounding lines of Filchner-Ronne and Ross ice shelves is reversible if they are allowed to regrow to their initial geometry. Overall, retreat of grounding lines in the ASE sector, in Filchner-Ronne and Ross ice shelves is found to be very sensitive to subtle changes in model parameters or ocean conditions while all other grounding lines remain at a steady state close to their current position in all present-day model configurations. An improved assessment of the predictive capabilities of large-scale ice sheet models over long timescales could help to reduce the range of admissible parameters and thereby uncertainties in the grounding line evolution. Further observations and coupled simulations of ice sheet and ocean models could help to provide a deeper analysis and to quantify the probability of large-scale retreat or committed instability today and under future warming. Importantly, committed instability means that a collapse is not irreversible yet; rather, the grounding lines are in a state of 'overshoot' – and if, and how fast, the collapse occurs in the future depends on how climate conditions evolve.

Appendix A: PICO

A1 Melt sensitivity for Filchner-Ronne Ice Shelf

We estimate the sensitivity of average melt rates to ocean warming for Filchner-Ronne Ice Shelf using an ocean model simulation described in Naughten et al. (2021). In the simulation a coupled setup of the ocean model MITgcm (Marshall et al., 1997; Losch, 2008) and the ice-sheet model Úa (Gudmundsson et al., 2012) for the Weddell Sea is forced by an abrupt quadrupling of CO2 in the atmosphere. Antarctic surface and oceanic boundary conditions are provided by UKESM (Met Office Hadley Centre (2019), 5.4.2022). We use the 'abrupt-4xCO2' experiment from the standard CMIP6 protocol for UKESM, and repeat the last 10 years 5 times to extend the simulation to be 200 years long. In this simulation, the FRIS cavity undergoes a two-step response, first salinity decreases which also reduces melting, then warm Circumpolar Deep Water enters the cavity and

https://doi.org/10.5194/tc-2022-105
Preprint. Discussion started: 31 May 2022

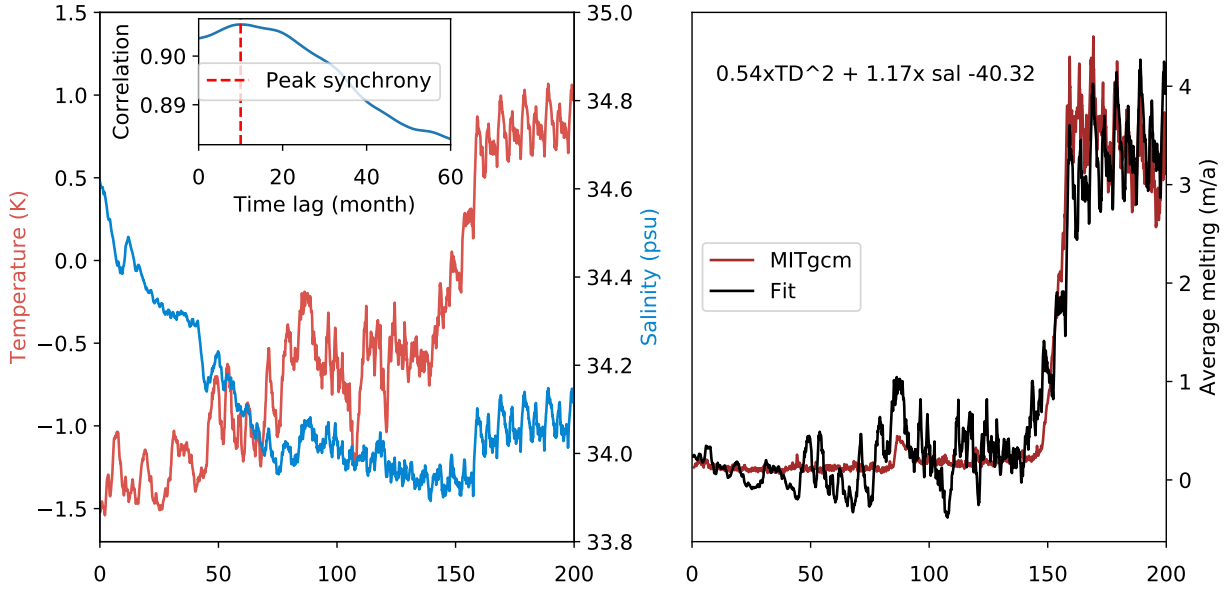

Figure A1. Filchner-Ronne Ice Shelf melt relationship estimate. Left panel: evolution of average ocean temperature and salinity at the depth of the continental shelf in front of the ice shelf in the ocean simulations of the Weddell Sea in Naughten et al. (2021) for the abrupt quadrupling of CO2. Inset shows correlation values for estimating the time-lag between shelf-wide averaged melt and ocean temperatures on the continental shelf. Right panel: modelled and predicted melt rates using the fitted function with parameters described in the figure.

drives an order of magnitude increase in melting, see Fig. A1. As this simulation spans a wide range of basal melt and ocean temperature forcing, we use it to derive the melt sensitivity of FRIS.

To this aim, we relate temperatures at the depth of the continental shelf in MITgcm with melting at the ice ocean interface. Using the average temperature over continental shelf in front of FRIS is a rough assumption which neglects complex processes that influence the in- and outflow of water masses in that cavity. However, it reflects best the assumptions and forcing used in PICO. First, we estimate the time the water masses on the continental shelf need to circulate into the cavity to drive melting using a cross-correlation. We find that a time-lag of 10 months yields the highest correlation between the temperature signal and the melt signal, see inset in Fig. A1. Then, we fit a function to the modelled data of thermal driving, salinity and melt rates using least-squares. We expect the melt rates to also depend on salinity because the salinity gradient between the continental shelf and the cavity controls the strength of circulation, which in turn affects the melt rate. We assume that the (time-shifted) melt depends quadratically on thermal driving (as discussed in Section 3.2) and linearly on salinity. Note that we assume a linear dependency on salinity as we are not aware of a more specific functional relationship. The R-squared value of the fit is 0.937 and the P-values for the coefficients are smaller than 0.0005, so we consider this sufficiently good. The resulting, predicted melt rates show a similar pattern of increase as the modelled melt rates, see right panel of Fig. A1. Differences arise since this fit cannot capture the complicated physical processes in the Weddell Sea. This also shows when we use the fitted relationship to predict melt in the alternative scenario from Naughten et al. (2021) that is based on a 1 percent increase in

https://doi.org/10.5194/tc-2022-105
Preprint. Discussion started: 31 May 2022


The Cryosphere Discussions
Open Access
EGU

Table A1. Baseline thermal driving for FRIS and the ASE region. Values are relative to the surface freezing point.

	$TD_{mean}(^{\circ}\mathrm{C})$	$TD_{min}(^{\circ}\mathrm{C})$	$TD_{max}(^{\circ}\mathrm{C})$	Citation
FRIS 4xCO2 (first 30 years)	0.53	0.35	0.84	Naughten et al. (2021)
FRIS historic	0.26	0.13	0.47	Naughten et al. (2021)
FRIS observations	0.14			Schmidtko et al. (2014)
PIG observations	1.85	1.42	2.22	Dutrieux et al. (2014)
DIS observations	1.38	1.04	1.84	Jenkins et al. (2018)
ASE observations	2.34			Schmidtko et al. (2014)

FRIS = Filchner Ronne Ice Shelf, PIG = Pine Island Glacier Ice Shelf, DIS = Dotson Ice Shelf, ASE = Amundsen Sea Embayment sector.

CO2, see Fig. S5. While we can capture about the order of magnitude of melt rate increase, the fitted model amplifies the trend in melting too much and produces too large variability. Also in the end of the abrupt quadrupling of CO2 (after year 160), the fitted function predicts increasing melt rates, because temperature and salinity slightly increase, while modeled melt rates slightly decrease. However, the fit is able to reproduce the large-scale pattern of the melt increase.

A2 Selection of baseline temperatures

We here describe the selection of baseline thermal driving (temperatures relative to the surface freezing point) to linearise the sensitivity between the selected thermal driving value and a warming of 1 K. The linearised sensitivity hence applies to current ocean temperatures and captures also a warming of around 1 K. While a sensitivity that is linearised around present-day (plus minus half a degree or going one degree below present-day) would be better suited for the historic simulations carried out in this paper, the increase from present-day levels was chosen since the numerical stability analysis of present-day grounding lines in the companion paper (Urruty et al., subm.) is tested by increasing ocean temperatures above present-day levels. It also makes the sensitivity estimates suitable for projections of the Antarctic sea-level contribution over the coming century. Note that if ocean temperatures change by more than one degree, for example in simulations over longer time scales, the quadratic relationship implies that PICO, which has a linear relationship, underestimates melt rate changes.

Table A1 shows a compilation of thermal driving values from modelling and observations. For FRIS, we list the min, mean and max of the first 30 years of the 4xCO2 simulation with low melt rates and conditions comparable to present-day, the historic simulation from 1979 to 2014 and the value from Schmidtko et al. (2014) as given in Reese et al. (2018a). For the Amundsen Sea, we use the min and max from the observations for PIG and DIS together with the value from Schmidtko et al. (2014) as given in Reese et al. (2018a).

We use the minimum and maximum of all values for an upper and lower range of sensitivities. For the best estimate of FRIS, we use the mean of the FRIS 4xCO2 simulation which is $0.53^{\circ}\mathrm{C}$. This makes the baseline thermal driving consistent with the fitted sensitivity curve. It is warmer than the average from the data in Schmidtko et al. (2014), so yields a slightly larger sensitivity, which is however still smaller than sensitivities estimated from other studies, see Sect. 3.2. For the best estimate

https://doi.org/10.5194/tc-2022-105
Preprint. Discussion started: 31 May 2022

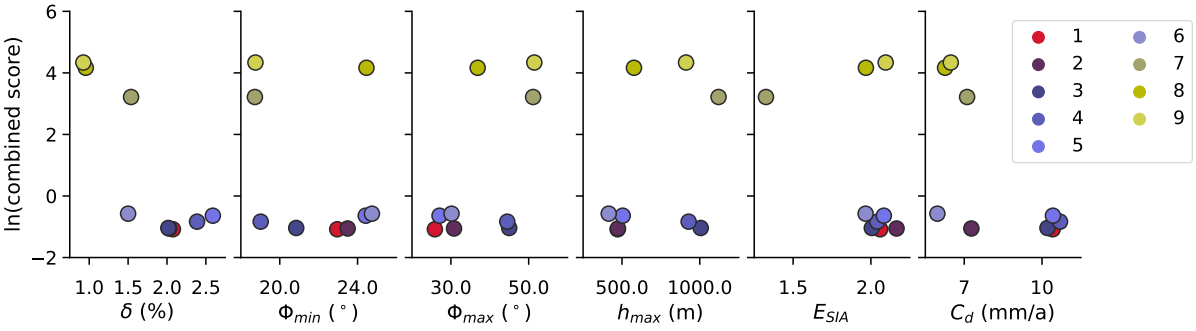

Figure B1. Scoring of ensemble of initial configurations in 2015. Scores are based on observed ice thickness, velocities, mass loss, grounding line positions, and a special focus is given to the Amundsen, Ross and Weddell seas. Initial ensemble members were obtained from equilibrium simulations of a full parameter ensemble with the best five runs for the entire AIS, the Amundsen, Weddell and Ross seas continued after 5000 to full 25,000 years (total of 16 runs). From these 9 runs were selected and for each a historic simulation was run from 1850 to 2015. The 2015 state is then scored with present-day observations. Shown is the natural logarithm of the scores. The lower the values the better the agreement with present-day.

in the ASE region, we use an average over available observational temperatures for DIS, PIG and the whole region, which is 1.65°C. This value is lower than the estimate in Schmidtko et al. (2014) and hence the sensitivity is slightly lower. It is however in line with sensitivity estimates from other studies, see Sect. 3.2, and the higher value is included as the maximum sensitivity estimate.

Appendix B: PISM simulations

We show the scoring for the initial configurations in 2015 (Fig. B1), and the long-term evolution of the control simulations (Fig. B2).

Code availability. PISM code is publicly available at https://github.com/pism/pism (last access: 5.4.2022). We plan to submit PISM simulations and python plotting scripts to the open access repository zenodo if the manuscript gets published.

Author contributions. In cooperation with all members of the TiPACCs work package 2, RR designed the study, ran the simulations with PISM and wrote the manuscript. JG supported the simulations and plotting. KN provided and processed the FRIS ocean model simulation data used for fitting the quadratic sensitivity curve. All authors contributed to the writing and discussion of ideas.

https://doi.org/10.5194/tc-2022-105
Preprint. Discussion started: 31 May 2022

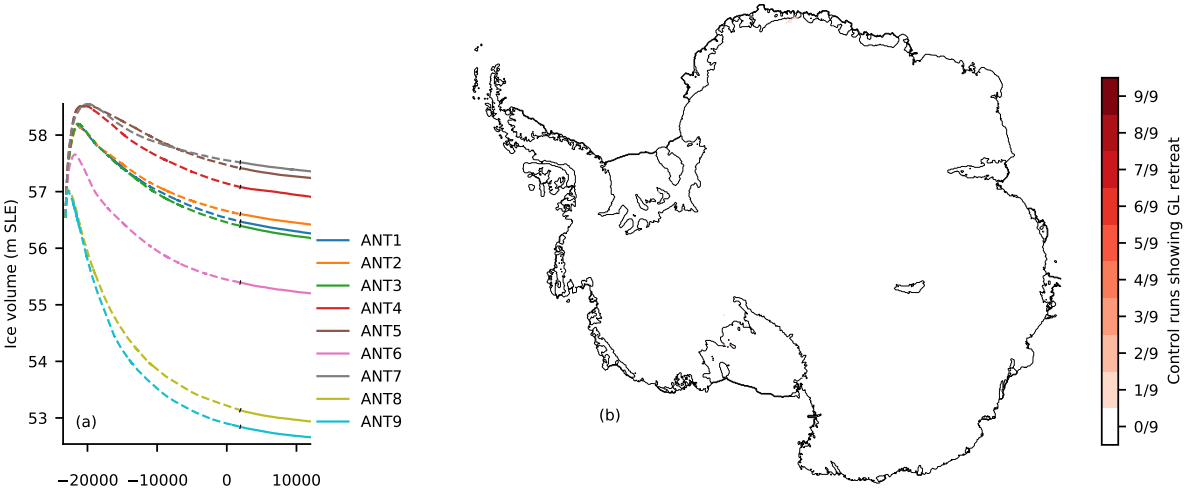

Figure B2. Control runs. Panel (a) shows the evolution of Antarctic Ice Sheet volume (in meters sea-level equivalent, m SLE) during the control runs for all ensemble members used in the manuscript. Black dots show historic control from 1850 to 2015. Panel (b) shows the regions that unground in the control runs between 1850 and year 12,000. The grey line is the BedMachine grounding line.

Competing interests. All authors declare that they have no competing interests.

Acknowledgements. This work is part of the TiPACCs project, which receives funding from the European Union's Horizon 2020 research and innovation programme under grant agreement no. 820575. Development of PISM is supported by NASA grant NNX17AG65G and NSF grants PLR-1603799 and PLR-1644277. The authors gratefully acknowledge the European Regional Development Fund (ERDF), the German Federal Ministry of Education and Research and the Land Brandenburg for supporting this project by providing resources on the high performance computer system at the Potsdam Institute for Climate Impact Research.

We would like to thank Christian Schoof for providing helpful input on stability analysis and Chris Bull and Adrian Jenkins for helpful discussions on the PICO parameter selection.

https://doi.org/10.5194/tc-2022-105
Preprint. Discussion started: 31 May 2022

References

Adusumilli, S., Fricker, H. A., Medley, B., Padman, L., and Siegfried, M. R.: Interannual variations in meltwater input to the Southern Ocean from Antarctic ice shelves, Nature Geoscience, 13, 616–620, https://doi.org/10.1038/s41561-020-0616-z, 2020.

Albrecht, T., Winkelmann, R., and Levermann, A.: Glacial-cycle simulations of the Antarctic Ice Sheet with the Parallel Ice Sheet Model (PISM)–Part 2: Parameter ensemble analysis, The Cryosphere, 14, 633–656, 2020.

Arthern, R. J. and Williams, C. R.: The sensitivity of West Antarctica to the submarine melting feedback, Geophysical Research Letters, 44, 2352–2359, 2017.

Aschwanden, A., Bueler, E., Khroulev, C., and Blatter, H.: An enthalpy formulation for glaciers and ice sheets, Journal of Glaciology, 58, 441–457, 2012.

Barthel, A., Agosta, C., Little, C. M., Hattermann, T., Jourdain, N. C., Goelzer, H., Nowicki, S., Seroussi, H., Straneo, F., and Bracegirdle, T. J.: CMIP5 model selection for ISMIP6 ice sheet model forcing: Greenland and Antarctica, The Cryosphere, 14, 855–879, 2020.

Bentsen, M., Bethke, I., Debernard, J. B., Iversen, T., Kirkevåg, A., Seland, Ø., Drange, H., Roelandt, C., Seierstad, I. A., Hoose, C., et al.: The Norwegian earth system model, NorESM1-M—Part 1: Description and basic evaluation of the physical climate, Geosci. Model Dev, 6, 687–720, 2013.

Brondex, J., Gagliardini, O., Gillet-Chaulet, F., and Durand, G.: Sensitivity of grounding line dynamics to the choice of the friction law, Journal of Glaciology, 63, 854–866, 2017.

Brondex, J., Gillet-Chaulet, F., and Gagliardini, O.: Sensitivity of centennial mass loss projections of the Amundsen basin to the friction law, The Cryosphere, 13, 177–195, 2019.

Bueler, E. and Brown, J.: Shallow shelf approximation as a "sliding law" in a thermomechanically coupled ice sheet model, Journal of Geophysical Research: Solid Earth, 114, 1–21, https://doi.org/10.1029/2008JF001179, 2009.

Bueler, E. and van Pelt, W.: Mass-conserving subglacial hydrology in the Parallel Ice Sheet Model version 0.6, Geoscientific Model Development, 8, 1613–1635, 2015.

Burgard, C., Jourdain, N. C., Reese, R., Jenkins, A., and Mathiot, P.: An assessment of basal melt parameterisations for Antarctic ice shelves, The Cryosphere Discussions, pp. 1–56, 2022.

Comeau, D., Asay-Davis, X. S., Begeman, C. B., Hoffman, M. J., Lin, W., Petersen, M. R., Price, S. F., Roberts, A. F., Van Roekel, L. P., Veneziani, M., et al.: The DOE E3SM v1. 2 Cryosphere Configuration: Description and Simulated Antarctic Ice-Shelf Basal Melting, Journal of Advances in Modeling Earth Systems, 14, e2021MS002 468, 2022.

Dutrieux, P., Rydt, J. D., Jenkins, A., Holland, P. R., Ha, H. K., Lee, S. H., Steig, E. J., Ding, Q., Abrahamsen, E. P., and Schroder, M.: Strong Sensitivity of Pine Island Ice-Shelf Melting to Climatic Variability, Science, 343, 174–178, https://doi.org/10.1126/science.1244341, 2014.

Favier, L., Durand, G., Cornford, S., Gudmundsson, G., Gagliardini, O., Gillet-Chaulet, F., Zwinger, T., Payne, A., and Le Brocq, A.: Retreat of Pine Island Glacier controlled by marine ice-sheet instability, Nature Climate Change, 4, 117–121, https://doi.org/doi:10.1038/nclimate2094, 2014.

Feldmann, J. and Levermann, A.: Collapse of the West Antarctic Ice Sheet after local destabilization of the Amundsen Basin, Proceedings of the national academy of sciences, 112, 14 191–14 196, 2015.

Feldmann, J. and Levermann, A.: From cyclic ice streaming to Heinrich-like events: the grow-and-surge instability in the Parallel Ice Sheet Model, The Cryosphere, 11, 1913–1932, 2017.

https://doi.org/10.5194/tc-2022-105
Preprint. Discussion started: 31 May 2022

Feldmann, J., Albrecht, T., Khroulev, C., Pattyn, F., and Levermann, A.: Resolution-dependent performance of grounding line motion in a shallow model compared with a full-Stokes model according to the MISMIP3d intercomparison, Journal of Glaciology, 60, 353–360, 2014.

Garbe, J., Albrecht, T., Levermann, A., Donges, J. F., and Winkelmann, R.: The hysteresis of the Antarctic ice sheet, Nature, 585, 538–544, 2020.

Golledge, N. R., Clark, P. U., He, F., Dutton, A., Turney, C., Fogwill, C., Naish, T., Levy, R. H., McKay, R. M., Lowry, D. P., et al.: Retreat of the Antarctic Ice Sheet during the Last Interglaciation and implications for future change, Geophysical Research Letters, 48, e2021GL094 513, 2021.

Gomez, N., Mitrovica, J. X., Huybers, P., and Clark, P. U.: Sea level as a stabilizing factor for marine-ice-sheet grounding lines, Nature Geoscience, 3, 850–853, 2010.

Gomez, N., Pollard, D., and Holland, D.: Sea-level feedback lowers projections of future Antarctic Ice-Sheet mass loss, Nature communications, 6, 1–8, 2015.

Gudmundsson, G.: Ice-shelf buttressing and the stability of marine ice sheets, The Cryosphere, 7, 647–655, 2013.

Gudmundsson, G. H., Krug, J., Durand, G., Favier, L., and Gagliardini, O.: The stability of grounding lines on retrograde slopes, The Cryosphere, 6, 1497–1505, https://doi.org/10.5194/tc-6-1497-2012, 2012.

Haseloff, M. and Sergienko, O. V.: The effect of buttressing on grounding line dynamics, Journal of Glaciology, 64, 417–431, 2018.

Hellmer, H. H., Kauker, F., Timmermann, R., Determann, J., and Rae, J.: Twenty-first-century warming of a large Antarctic ice-shelf cavity by a redirected coastal current, Nature, 485, 225–228, 2012.

Hellmer, H. H., Kauker, F., Timmermann, R., and Hattermann, T.: The fate of the southern Weddell Sea continental shelf in a warming climate, Journal of Climate, 30, 4337–4350, 2017.

Hoffman, M. J., Asay-Davis, X., Price, S. F., Fyke, J., and Perego, M.: Effect of subshelf melt variability on sea level rise contribution from Thwaites Glacier, Antarctica, Journal of Geophysical Research: Earth Surface, 124, 2798–2822, 2019.

Holland, P. R., Jenkins, A., and Holland, D. M.: The Response of Ice Shelf Basal Melting to Variations in Ocean Temperature, Journal of Climate, 21, 2558–2572, https://doi.org/10.1175/2007jcli1909.1, 2008.

Holland, P. R., Bracegirdle, T. J., Dutrieux, P., Jenkins, A., and Steig, E. J.: West Antarctic ice loss influenced by internal climate variability and anthropogenic forcing, Nature Geoscience, 12, 718–724, 2019.

Hughes, T. P., Linares, C., Dakos, V., Van De Leemput, I. A., and Van Nes, E. H.: Living dangerously on borrowed time during slow, unrecognized regime shifts, Trends in ecology & evolution, 28, 149–155, 2013.

Jenkins, A.: A one-dimensional model of ice shelf-ocean interaction, Journal of Geophysical Research: Oceans, 96, 20 671–20 677, https://doi.org/10.1029/91JC01842, 1991.

Jenkins, A., Dutrieux, P., Jacobs, S., Steig, E. J., Gudmundsson, G. H., Smith, J., and Heywood, K. J.: Decadal ocean forcing and Antarctic ice sheet response: Lessons from the Amundsen Sea, Oceanography, 29, 106–117, 2016.

Jenkins, A., Shoosmith, D., Dutrieux, P., Jacobs, S., Kim, T. W., Lee, S. H., Ha, H. K., and Stammerjohn, S.: West Antarctic Ice Sheet retreat in the Amundsen Sea driven by decadal oceanic variability, Nature Geoscience, 11, 733–738, https://doi.org/10.1038/s41561-018-0207-4, 2018.

Joughin, I., Smith, B. E., and Medley, B.: Marine ice sheet collapse potentially under way for the Thwaites Glacier Basin, West Antarctica, Science, 344, 735–738, 2014.

https://doi.org/10.5194/tc-2022-105
Preprint. Discussion started: 31 May 2022

Jourdain, N. C., Asay-Davis, X., Hattermann, T., Straneo, F., Seroussi, H., Little, C. M., and Nowicki, S.: A protocol for calculating basal melt rates in the ISMIP6 Antarctic ice sheet projections, The Cryosphere, 14, 3111–3134, https://doi.org/10.5194/tc-14-3111-2020, 2020.

Langebroek, P. M., Paul, A., and Schulz, M.: Antarctic ice-sheet response to atmospheric CO 2 and insolation in the Middle Miocene, Climate of the Past, 5, 633–646, 2009.

Losch, M.: Modeling ice shelf cavities in azcoordinate ocean general circulation model, Journal of Geophysical Research, 113, https://doi.org/10.1029/2007jc004368, 2008.

Marshall, J., Hill, C., Perelman, L., and Adcroft, A.: Hydrostatic, quasi-hydrostatic, and nonhydrostatic ocean modeling, Journal of Geophysical Research: Oceans, 102, 5733–5752, https://doi.org/10.1029/96jc02776, 1997.

Martin, M. A., Winkelmann, R., Haseloff, M., Albrecht, T., Bueler, E., Khroulev, C., and Levermann, A.: The Potsdam Parallel Ice Sheet Model (PISM-PIK) – Part 2: Dynamic equilibrium simulation of the Antarctic ice sheet, The Cryosphere, 5, 727–740, https://doi.org/10.5194/tc-5-727-2011, 2011.

Mengel, M. and Levermann, A.: Ice plug prevents irreversible discharge from East Antarctica, Nature Climate Change, 4, 451–455, 2014.

Mercer, J. H.: West Antarctic ice sheet and CO 2 greenhouse effect: a threat of disaster, Nature, 271, 321–325, 1978.

Met Office Hadley Centre (2019): WCRP CMIP6: Met Office Hadley Centre (MOHC) UKESM1-0-LL model output for the "abrupt-4xCO2" experiment, Centre for Environmental Data Analysis, 5.4.2022.

Milillo, P., Rignot, E., Rizzoli, P., Scheuchl, B., Mouginot, J., Bueso-Bello, J., Prats-Iraola, P., and Dini, L.: Rapid glacier retreat rates observed in West Antarctica, Nature Geoscience, pp. 1–6, 2022.

Morlighem, M., Rignot, E., Binder, T., Blankenship, D., Drews, R., Eagles, G., Eisen, O., Ferraccioli, F., Forsberg, R., Fretwell, P., et al.: Deep glacial troughs and stabilizing ridges unveiled beneath the margins of the Antarctic ice sheet, Nature Geoscience, 13, 132–137, 2020.

Mouginot, J., Rignot, E., and Scheuchl, B.: Continent-wide, interferometric SAR phase, mapping of Antarctic ice velocity, Geophysical Research Letters, 46, 9710–9718, 2019.

Naughten, K. A., Rydt, J. D., Rosier, S. H. R., Jenkins, A., Holland, P. R., and Ridley, J. K.: Two-timescale response of a large Antarctic ice shelf to climate change, Nature Communications, 12, https://doi.org/10.1038/s41467-021-22259-0, 2021.

Olbers, D. and Hellmer, H.: A box model of circulation and melting in ice shelf caverns, Ocean Dynamics, 60, 141–153, 2010.

Paolo, F. S., Fricker, H. A., and Padman, L.: Volume loss from Antarctic ice shelves is accelerating, Science, 348, 327–331, 2015.

Payne, A. J., Holland, P. R., Shepherd, A. P., Rutt, I. C., Jenkins, A., and Joughin, I.: Numerical modeling of ocean-ice interactions under Pine Island Bay's ice shelf, Journal of Geophysical Research, 112, https://doi.org/10.1029/2006jc003733, 2007.

Pegler, S. S.: Suppression of marine ice sheet instability, Journal of Fluid Mechanics, 857, 648–680, 2018.

Pollard, D. and DeConto, R. M.: Hysteresis in Cenozoic Antarctic ice-sheet variations, Global and Planetary Change, 45, 9–21, 2005.

Reese, R., Albrecht, T., Mengel, M., Asay-Davis, X., and Winkelmann, R.: Antarctic sub-shelf melt rates via PICO, The Cryosphere, 12, 1969–1985, https://doi.org/10.5194/tc-12-1969-2018, 2018a.

Reese, R., Winkelmann, R., and Gudmundsson, G. H.: Grounding-line flux formula applied as a flux condition in numerical simulations fails for buttressed Antarctic ice streams, The Cryosphere, 12, 3229–3242, 2018b.

Reese, R., Levermann, A., Albrecht, T., Seroussi, H., and Winkelmann, R.: The role of history and strength of the oceanic forcing in sea level projections from Antarctica with the Parallel Ice Sheet Model, The Cryosphere, 14, 3097–3110, https://doi.org/10.5194/tc-14-3097-2020, 2020.

Rignot, E., Mouginot, J., Morlighem, M., Seroussi, H., and Scheuchl, B.: Widespread, rapid grounding line retreat of Pine Island, Thwaites, Smith, and Kohler glaciers, West Antarctica, from 1992 to 2011, Geophysical Research Letters, 41, 3502–3509, 2014.

Rignot, E., Mouginot, J., Scheuchl, B., Van Den Broeke, M., Van Wessem, M. J., and Morlighem, M.: Four decades of Antarctic Ice Sheet mass balance from 1979–2017, Proceedings of the National Academy of Sciences, 116, 1095–1103, 2019.

Ritchie, P., Karabacak, Ö., and Sieber, J.: Inverse-square law between time and amplitude for crossing tipping thresholds, Proceedings of the Royal Society A, 475, 20180 504, 2019.

Ritchie, P. D., Clarke, J. J., Cox, P. M., and Huntingford, C.: Overshooting tipping point thresholds in a changing climate, Nature, 592, 517–523, 2021.

Rosier, S. H., Reese, R., Donges, J. F., De Rydt, J., Gudmundsson, G. H., and Winkelmann, R.: The tipping points and early warning indicators for Pine Island Glacier, West Antarctica, The Cryosphere, 15, 1501–1516, 2021.

Scheffer, M., Bascompte, J., Brock, W. A., Brovkin, V., Carpenter, S. R., Dakos, V., Held, H., Van Nes, E. H., Rietkerk, M., and Sugihara, G.: Early-warning signals for critical transitions, Nature, 461, 53–59, 2009.

Schmidtko, S., Heywood, K. J., Thompson, A. F., and Aoki, S.: Multidecadal warming of Antarctic waters, Science, 346, 1227–1231, https://doi.org/10.1126/science.1256117, 2014.

Schoof, C.: Ice sheet grounding line dynamics: Steady states, stability, and hysteresis, Journal of Geophysical Research: Earth Surface, 112, 2007.

Schoof, C.: Marine ice sheet stability, Journal of Fluid Mechanics, 698, 62, 2012.

Seroussi, H. and Morlighem, M.: Representation of basal melting at the grounding line in ice flow models, The Cryosphere, 12, 3085–3096, 2018.

Seroussi, H., Nakayama, Y., Larour, E., Menemenlis, D., Morlighem, M., Rignot, E., and Khazendar, A.: Continued retreat of Thwaites Glacier, West Antarctica, controlled by bed topography and ocean circulation, Geophysical Research Letters, 44, 6191–6199, https://doi.org/10.1002/2017gl072910, 2017.

Seroussi, H., Nowicki, S., Payne, A. J., Goelzer, H., Lipscomb, W. H., Abe-Ouchi, A., Agosta, C., Albrecht, T., Asay-Davis, X., Barthel, A., Calov, R., Cullather, R., Dumas, C., Galton-Fenzi, B. K., Gladstone, R., Golledge, N. R., Gregory, J. M., Greve, R., Hattermann, T., Hoffman, M. J., Humbert, A., Huybrechts, P., Jourdain, N. C., Kleiner, T., Larour, E., Leguy, G. R., Lowry, D. P., Little, C. M., Morlighem, M., Pattyn, F., Pelle, T., Price, S. F., Quiquet, A., Reese, R., Schlegel, N.-J., Shepherd, A., Simon, E., Smith, R. S., Straneo, F., Sun, S., Trusel, L. D., Breedam, J. V., van de Wal, R. S. W., Winkelmann, R., Zhao, C., Zhang, T., and Zwinger, T.: ISMIP6 Antarctica: a multi-model ensemble of the Antarctic ice sheet evolution over the 21st century, The Cryosphere, 14, 3033–3070, https://doi.org/10.5194/tc-14-3033-2020, 2020.

Shepherd, A., Ivins, E., Rignot, E., Smith, B., Van Den Broeke, M., Velicogna, I., Whitehouse, P., Briggs, K., Joughin, I., Krinner, G., et al.: Mass balance of the Antarctic Ice Sheet from 1992 to 2017, Nature, 558, 219–222, 2018.

Smith, B., Fricker, H. A., Gardner, A. S., Medley, B., Nilsson, J., Paolo, F. S., Holschuh, N., Adusumilli, S., Brunt, K., Csatho, B., et al.: Pervasive ice sheet mass loss reflects competing ocean and atmosphere processes, Science, 368, 1239–1242, 2020.

Strogatz, S. H.: Nonlinear dynamics and chaos: with applications to physics, biology, chemistry, and engineering, CRC press, 2018.

Sun, S., Pattyn, F., Simon, E. G., Albrecht, T., Cornford, S., Calov, R., Dumas, C., Gillet-Chaulet, F., Goelzer, H., Golledge, N. R., et al.: Antarctic ice sheet response to sudden and sustained ice-shelf collapse (ABUMIP), Journal of Glaciology, 66, 891–904, 2020.

Urruty, B., Hill, E., Reese, R., Garbe, J., Gagliardini, O., Durand, G., Gillet-Chaulet, F., Gudmundsson, G. H., Winkelmann, R., Chekki, M., Chandler, D., and Langebroek, P. M.: The stability of present-day Antarctic grounding lines — Part A: No indication of marine ice sheet instability in the current geometry, The Cryosphere, subm.

https://doi.org/10.5194/tc-2022-105
Preprint. Discussion started: 31 May 2022

van Wessem, J. M., van de Berg, W. J., Noël, B. P. Y., van Meijgaard, E., Amory, C., Birnbaum, G., Jakobs, C. L., Krüger, K., Lenaerts, J. T. M., Lhermitte, S., Ligtenberg, S. R. M., Medley, B., Reijmer, C. H., van Tricht, K., Trusel, L. D., van Ulft, L. H., Wouters, B., Wuite, J., and van den Broeke, M. R.: Modelling the climate and surface mass balance of polar ice sheets using RACMO2 – Part 2: Antarctica (1979–2016), Cryosphere, 12, 1479–1498, https://doi.org/10.5194/tc-12-1479-2018, 2018.

Vanselow, A., Halekotte, L., and Feudel, U.: Evolutionary rescue can prevent rate-induced tipping, Theoretical Ecology, 15, 29–50, 2022.

Weertman, J.: Stability of the junction of an ice sheet and an ice shelf, Journal of Glaciology, 13, 3–11, 1974.

Winkelmann, R., Martin, M. A., Haseloff, M., Albrecht, T., Bueler, E., Khroulev, C., and Levermann, A.: The Potsdam parallel ice sheet model (PISM-PIK)–Part 1: Model description, The Cryosphere, 5, 715–726, 2011.

Zeitz, M., Haacker, J. M., Donges, J. F., Albrecht, T., and Winkelmann, R.: Dynamic regimes of the Greenland Ice Sheet emerging from interacting melt-elevation and glacial isostatic adjustment feedbacks, Earth System Dynamics Discussions, pp. 1–25, 2021.